Multi-Patch Prediction: Adapting Language Models for Time Series Representation Learning

Yuxuan Bian [*1 2] Xuan Ju [*1] Jiangtong Li [*2] Zhijian Xu [1] Dawei Cheng [2] Qiang Xu [1]

Abstract

In this study, we present *aLLM4TS*, an innovative framework that adapts Large Language Models (LLMs) for time-series representation learning. Central to our approach is that we reconceive time-series forecasting as a self-supervised, multi-patch prediction task, which, compared to traditional mask-and-reconstruction methods, captures temporal dynamics in patch representations more effectively. Our strategy encompasses two-stage training: (i). a causal continual pre-training phase on various time-series datasets, anchored on next patch prediction, effectively syncing LLM capabilities with the intricacies of time-series data; (ii). fine-tuning for multi-patch prediction in the targeted time-series context. A distinctive element of our framework is the patch-wise decoding layer, which departs from previous methods reliant on sequence-level decoding. Such a design directly transposes individual patches into temporal sequences, thereby significantly bolstering the model's proficiency in mastering temporal patch-based representations. aLLM4TS demonstrates superior performance in several downstream tasks, proving its effectiveness in deriving temporal representations with enhanced transferability and marking a pivotal advancement in the adaptation of LLMs for time-series analysis.

1. Introduction

Time-series analysis (TSA) plays a pivotal role in a myriad of real-world applications. Current state-of-the-art TSA methodologies are usually custom-designed for specific tasks, such as forecasting (Zeng et al., 2023; Xu et al., 2024; Liu et al., 2022a; Nie et al., 2023), classification (Dempster et al., 2020), and anomaly detection (Xu et al., 2021).

[*]Equal contribution [1]The Chinese University of Hong Kong [2]Tongji University. Correspondence to: Dawei Cheng <dcheng@tongji.edu.cn>, Qiang Xu <qxu@cse.cuhk.edu.hk>.

Proceedings of the 41st International Conference on Machine Learning, Vienna, Austria. PMLR 235, 2024. Copyright 2024 by the author(s).

Despite these advancements, the quest for a versatile time-series representation capable of addressing diverse downstream tasks remains a formidable challenge. Traditional approaches predominantly rely on self-supervised learning strategies such as contrastive learning (Yue et al., 2022; Yang & Hong, 2022) and mask-and-reconstruction modeling (Zerveas et al., 2021; Li et al., 2023). Yet, they often struggle to fully grasp the intricate temporal variations characteristic of time series, arising from inconsistencies between high-level representation optimization with downstream low-level tasks (Xie et al., 2023), or the temporal disruption caused by random masking (Ma et al., 2023).

The advent of large language models (LLMs) has revolutionized the field of natural language processing (OpenAI, 2023; Brown et al., 2020). Their remarkable adaptability extends beyond text, as demonstrated through prompting or fine-tuning for various modalities (Lu et al., 2023; Borsos et al., 2023). This adaptability has sparked a surge of interest in leveraging LLMs for TSA. Some studies have explored the use of frozen LLMs in TSA, either through the artful design of prompts (Gruver et al., 2024; Yu et al., 2023; Xue & Salim, 2023) or by reprogramming input time-series (Jin et al., 2024; Cao et al., 2024). Others have experimented with fine-tuning LLMs for specific TSA tasks (Zhou et al., 2023; Chang et al., 2023; Sun et al., 2024). While these methods show promise, they tend to fall short in generating a comprehensive time-series representation due to implicit representation adaption and inappropriate sequence-wise decoder (Spathis & Kawsar, 2023; Lee et al., 2023) in Fig. 1.

Recognizing the potential of LLMs in time-series modeling and the shortcomings of the aforementioned methods, we present *aLLM4TS*, an innovative framework that fully realizes the potential of LLMs for general time-series representation learning. Our framework reconceptualizes time-series forecasting as a self-supervised, multi-patch[1] prediction task. This approach offers a more effective mechanism for capturing temporal dynamics at the patch level, mitigates the modeling inconsistency in contrastive learning and the temporal dependencies disruption in mask-and-reconstruction,

[1]The patch concept, introduced by Nie et al. (2023), denotes the segmentation of the original time series at the subseries level, serving as input tokens for transformer-based TSA models.

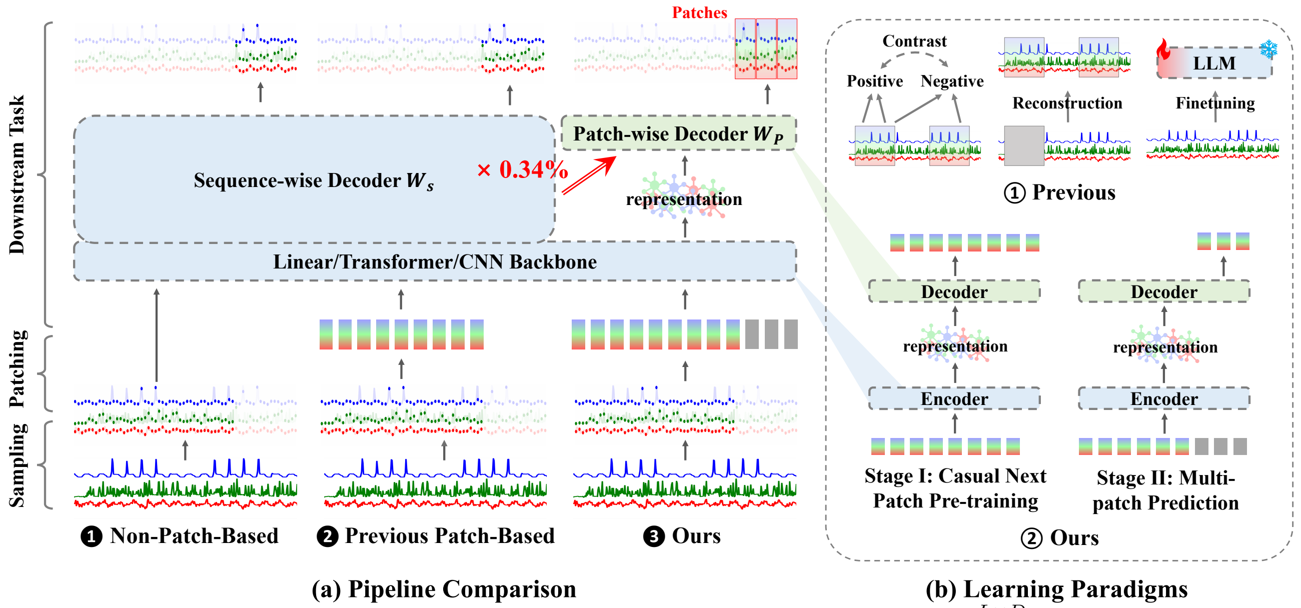

Figure 1: **Pipeline Comparison.** Given a time series embedding/patch sequence $\boldsymbol{x} \in \mathbb{R}^{L \times D}, D \gg P$ where P is the patch size and forecasting horizon H: Non-Patch Based Models ❶ or Patch Based Models ❷ map it to the target sequence using a huge sequence-level linear layer $\mathbf{W}_s \in \mathbb{R}^{(L \cdot D) \times H}$; Our Patch-based Parallel Decoding aLLM4TS ❸ decodes each patch to the time domain using a small shared patch-level linear layer $\mathbf{W}_p \in \mathbb{R}^{D \times P}$ without modeling temporal relationships among patches. Specifically, the parameters of our patch-based decoding layer are only $\frac{P}{L * H}$ (*e.g.*, 0.34%, when $P = 16, L = 64, H = 720$), compared to the sequence-based decoding layer. **Learning Paradigms.** Instead of contrastive learning, masking reconstruction, and limited fine-tuning of the LLMs ①, we adopt a forecasting-based two-stage pre-training task ② to better transfer the sequence modeling capabilities within LLMs to time series.

and aligns with the casual pre-training process of LLMs.

Specifically, we implement a two-stage self-supervised training strategy to tailor LLMs for time-series representation learning. The first stage involves causal continual training on a variety of time-series datasets, focusing on next-patch prediction to synchronize LLM capabilities with time-series data intricacies. The subsequent stage involves fine-tuning the model for multi-patch prediction in targeted time-series scenarios. A pivotal aspect of our framework is the innovative design of the patch-wise decoder (depicted in Figure 1). This design mandates the model to decode each patch independently into temporal sequences, deviating from the conventional sequence-wise decoding approach, thus enabling the encoding of time-series representations directly within patches as the decoder is precluded from using the patch sequence for temporal dynamics modeling.

In summary, the primary contributions of this work include:

- We introduce *aLLM4TS*, an innovative framework adapting LLMs for patch-based time-series representation learning. This framework utilizes a two-stage forecasting-based pre-training strategy. The first stage encompasses causal next-patch training, transferring LLM capabilities for nuanced understandings of time-series data, followed by a fine-tuning stage focused on multi-patch prediction, ensuring a robust representation adaptation to specific time-series contexts.
- Diverging from traditional approaches that utilize sequence-wise decoding in TSA tasks, we propose a novel patch-wise decoding methodology. This approach significantly improves the adaptability of LLM backbones, optimizing patch-based time-series representation learning more effectively.
- *aLLM4TS*[2] demonstrates superior performance across a variety of downstream TSA tasks and across diverse data domains, validating its ability to derive time-series representations with remarkable transferability and setting new benchmarks in the field.

2. Related Work

2.1. Time Series Representation Learning

The field of time series representation learning has witnessed increasing interest in recent years, with self-supervised learning methods playing a pivotal role. These methods generally fall into two categories:

Contrastive Learning. This category encompasses methods designed to refine the representation space by leveraging various forms of consistency, such as subseries consistency (Franceschi et al., 2019; Fortuin et al., 2019), temporal consistency (Tonekaboni et al., 2021; Woo et al., 2022a;

[2]Code is available at https://github.com/yxbian23/aLLM4TS

Yue et al., 2022), transformation consistency (Zhang et al., 2022b; Yang & Hong, 2022), and contextual consistency (Eldele et al., 2021). The goal is to ensure that representations of positive pairs are closely aligned, whereas those of negative pairs are distinctly separated. Despite their strengths, contrastive learning methods often struggle with aligning to low-level tasks such as forecasting, primarily due to their focus on high-level information (Xie et al., 2023).

Masked Modeling. PatchTST (Nie et al., 2023) pioneers the utilization of patches as the basic unit for processing time series, advocating for the prediction of masked subseries-level patches to grasp local semantic information while minimizing memory consumption. However, this approach tends to compromise temporal dependencies and fails to guarantee adequate representation learning of temporal dynamics, as the masked values are often predictably inferred from adjacent contexts (Li et al., 2023).

2.2. Time Series Analysis based on LLMs

The adaptation of pre-trained LLMs for time series analysis has garnered significant attention, exploiting their exceptional ability in sequence representation learning. This body of work can be categorized into three primary approaches:

- **Zero-shot Adaptation.** Studies such as those by Gruver et al. (2024); Xue & Salim (2023); Yu et al. (2023) leverage the inherent sequence representation capabilities of frozen LLMs to facilitate time series prediction without any task-specific training.
- **Prompt Optimization.** Works by Jin et al. (2024); Cao et al. (2024); Sun et al. (2024) employ reprogrammed input time series in conjunction with the innate sequence modeling prowess of pre-trained LLMs, aiming for enhanced forecasting accuracy.
- **Limited Fine-tuning.** Research efforts like those of Zhou et al. (2023); Liu et al. (2023); Chang et al. (2023) apply fine-tuning to selected components of LLMs to improve performance in time series analysis tasks.

While these approaches yield encouraging outcomes, they predominantly focus on distinct TSA tasks, instead of achieving a holistic time-series representation.

3. Preliminaries and Motivation

3.1. Preliminaries

Time-Series Forecasting (TSF) is the fundamental challenge in time series analysis (Ma et al., 2023), aiming to analyze the dynamics and correlations among historical time-series data to predict future behavior, formulated as:

$$P(\mathbf{x}_i^{L+1:L+H}|\mathbf{x}_i^{1:L}) = \prod_{t=L+1}^{L+H} P(x_i^t|\mathbf{x}_i^{1:t-1}) \qquad (1)$$

where L is the look-back window size and x_i^t is the value of the i_{th} variate at the t_{th} time step, and the modeling target is to learn the unknown distribution of the H future values.

Casual Language Model Pre-training. Current LLMs mostly belong to casual language models (OpenAI, 2023; Radford et al., 2019). They utilize a diagonal masking matrix, ensuring that each token can only access information from previous tokens. The training objective is to predict the next token based on the history information, defined as:

$$\mathcal{L}_{CLM} = \sum_{i=2}^{N} \log P(\mathbf{x}_i|\mathbf{x}_1, \cdots, \mathbf{x}_{i-1}) \qquad (2)$$

where N is the number of tokens, $\mathbf{x}_i$ denotes the i-th token.

3.2. Motivation

We explain the motivation of our proposed aLLM4TS solution by raising and answering the following two questions.

How can we effectively adapt LLMs in time series modality? Traditional contrastive learning $\mathcal{L}_{CL}$ and mask-and-reconstruction $\mathcal{L}_{MR}$ serve as a training loss, defined as:

$$\begin{aligned}\mathcal{L}_{CL} &= -\frac{1}{N}\sum_{i=1}^{N}\log\frac{\exp(f(\mathbf{x}_i)^{\mathrm{T}}f(\mathbf{x}_i^p))}{\exp(f(\mathbf{x}_i)^{\mathrm{T}}f(\mathbf{x}_i^p)) + \sum_{j=1}^{B-1}\exp(f(\mathbf{x}_i)^{\mathrm{T}}f(\mathbf{x}_i^j))},\\ \mathcal{L}_{MR} &= \sum_{i=1}^{N}\|\mathbf{x}_i - \widehat{\mathbf{x}}_i\|_2^2 = \sum_{i=1}^{N}\|\mathbf{x}_i - f(\mathrm{Mask}(\mathbf{x}_i))\|_2^2,\end{aligned} \qquad (3)$$

where N denotes the number of training samples (pairs), $B-1$ is the number of negative samples, $\mathbf{x}_i$ denotes the i-th sample, $\mathbf{x}_i^p$ is the only positive sample, $\mathbf{x}_i^j$ is the j-th negative sample of $\mathbf{x}_i$, $\widehat{\mathbf{x}}_i$ is the corresponding masked sample, $f(\cdot)$ is the forward pass. Both are inappropriate for adapting LLMs into time series since the non-negligible misalignment between their modeling objective with time series modeling and casual sequence pre-training processes of LLMs (Xie et al., 2023; Dong et al., 2023). However, during the pre-training stages in Eq. 2, casual LLMs undergo a similar training process as TSF in Eq. 1 on massive tokens (Brown et al., 2020; Radford et al., 2019), where x_i^t is the t_{th} token of the i_{th} sentences. This drives us to reformulate time-series forecasting as a self-supervised multi-patch prediction task. This offers several benefits: (1) **Guarantee modeling consistency** between high-level representation optimization and downstream low-level tasks, where contrastive learning fails, fostering a versatile representation with robust predictive capabilities excelling in diverse TSA tasks. (2) **Avoid the temporal dependencies disruption** caused by random masking in masked modeling. (3) **Align with LLMs' pre-training** where each token is casually predicted, facilitating the seamless adaptation of LLM to the temporal domain. Thus, we devise a forecasting-based self-supervised training strategy, as in Fig. 2 (a) and (b), to naturally sync LLMs' excellent representation learning capabilities with time-series variations, including a casual

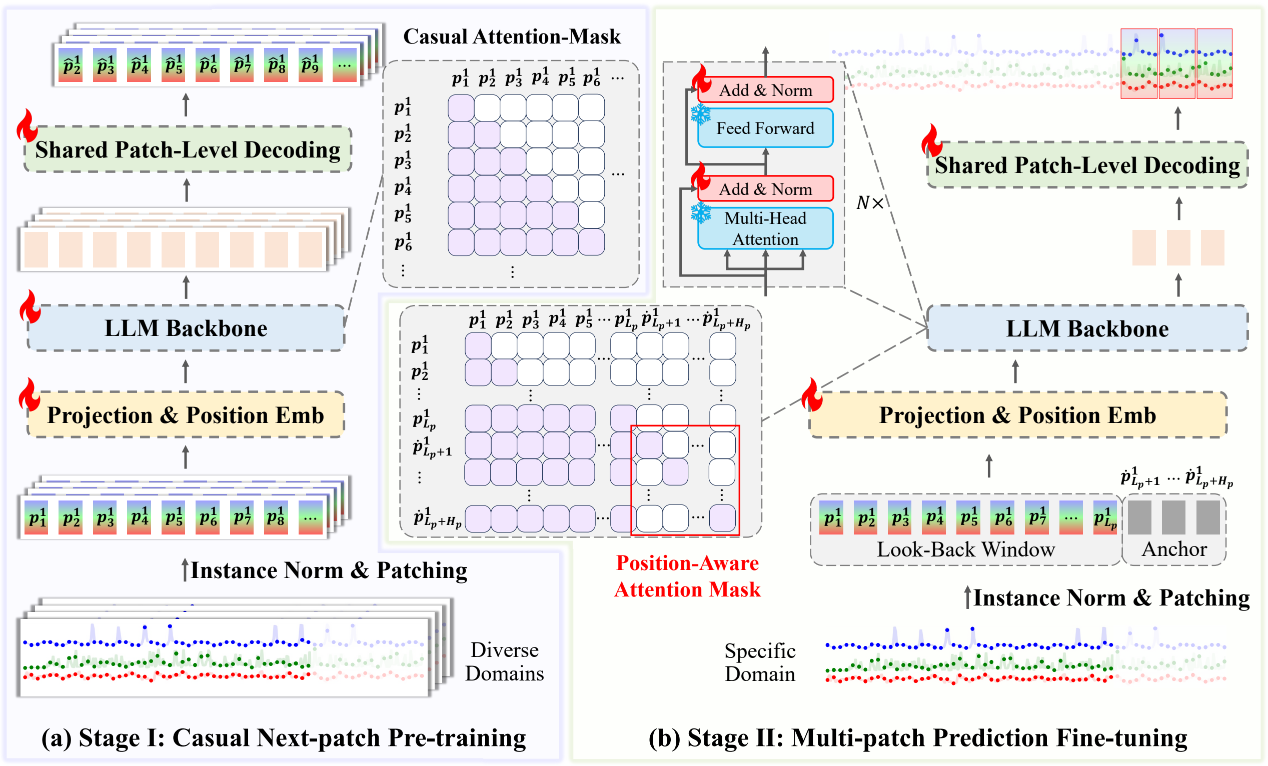
Casual Attention-Mask
Shared Patch-Level Decoding
LLM Backbone
Projection & Position Emb
Instance Norm & Patching
Diverse Domains
(a) Stage I: Casual Next-patch Pre-training
Add & Norm
Feed Forward
Add & Norm
Multi-Head Attention
N×
Position-Aware Attention Mask
Look-Back Window
Anchor
Specific Domain
(b) Stage II: Multi-patch Prediction Fine-tuning

Figure 2: **The model framework of aLLM4TS**. In stage 1, **Casual Next-patch Pre-training (a)**, time series from different datasets are initially converted into univariate patch sequences. Then, we conduct next-patch prediction training with casual attention, effectively syncing LLM capabilities with the intricacies of time-series data. In stage 2, **Multi-patch Prediction Fine-tuning (b)**, we fine-tune a few layers for multi-patch prediction in the target time-series context. Firstly, non-parametric methods are first employed to obtain the initial anchor representation of the horizon. Next, we concatenate the look-back window patches and anchors and feed them into the time-series-aligned LLM after stage 1 training with a position-aware attention mask, optimizing anchors with history patches. Finally, all optimized horizon anchors are independently decoded into the target temporal domain through a shared patch-wise linear decoder.

next-patch continual pre-training and a fine-tuning for multi-patch prediction in the target time-series context.

Is the sequence-level decoder suitable for patch-based time series representation? Current TSA models based on LLMs (Jin et al., 2024; Zhou et al., 2023) follow the traditional patch-based framework in Fig. 1 ❷. Given patch-based time series representation $\{\boldsymbol{p}_1, \cdots, \boldsymbol{p}_{L_p}\}, \boldsymbol{p}_i \in \mathbb{R}^D$ across L_p patches with dimension D, they concatenate and map the patch sequence to prediction horizon H_p, through a sequence-level decoder $\mathbf{W}_s \in \mathbb{R}^{(L_p \cdot D) \times H_p}$, which can be particularly oversized if either one or all of these values are large, causing severe downstream task overfitting. Instead of mapping at the sequence level, we disentangle the encoding and decoding within our framework through a patch-wise decoder in Fig. 1 ❸, which is involved throughout our pipeline (Stage 1 and Stage 2). This empowers the LLM backbone and patch-wise decoder to excel in its designated role: encoding each patch for better representation and decoding each patch independently to the temporal domain.

4. Method

Our aLLM4TS stands as a novel framework in redefining the landscape of adapting LLMs into time series analysis.

4.1. Casual Next-patch Continual Pre-Training

In this section, we propose to conduct casual next-patch continual pre-training, to sync pre-trained LLMs sequence modeling capabilities with time-series modalities on diverse time series datasets(e.g., Weather, Traffic), as in Fig. 2 (a).

Forward Process. Given time series from various datasets, we first flatten them into M univariate sequences. We denote the i-th univariate series of look-back window size L starting at time index t as $\boldsymbol{x}_{t:t+L-1}^{(i)} = \{x_t^{(i)}, ..., x_{t+L-1}^{(i)}\} \in \mathbb{R}^{1\times L}$ where $i = 1, ..., M$. Then each of them is first divided into patch sequence $\boldsymbol{p}_{t_p:t_p+L_p-1}^{(i)} = \{\boldsymbol{p}_{t_p}^{(i)}, ..., \boldsymbol{p}_{t_p+L_p-1}^{(i)}\} \in \mathbb{R}^{L_p \times P}$ where $t_p = \lfloor\frac{(t-P)}{S}\rfloor + 1$ is starting patch index, $L_p = \lfloor\frac{(L-P)}{S}\rfloor + 1$ is the number of patches, P is the patch length, and S is the sliding stride. Finally, each sequence is fed independently into the casual LLM backbone, such as GPT2 (Radford et al., 2019) for the channel-independence setting. Then we get the casual next-patch prediction $\hat{\boldsymbol{p}}^{(i)}_{t_p+1:t_p+L_p} = \{\hat{\boldsymbol{p}}^{(i)}_{t_p+1}, ..., \hat{\boldsymbol{p}}^{(i)}_{t_p+L_p}\} \in \mathbb{R}^{L_p \times D}$.

Loss Function. We choose to use the MSE loss to guide the representation alignment at the patch level. The loss in each time series is gathered and averaged over M time series to get the overall objective loss: $\mathcal{L}_p = \mathbb{E}_{\boldsymbol{p}} \frac{1}{M} \sum_{i=1}^{M} \|\hat{\boldsymbol{p}}^{(i)}_{t_p+1:t_p+L_p} - \boldsymbol{p}^{(i)}_{t_p+1:t_p+L_p}\|_2^2$, which is employed to guide the casual next-patch time-series representation optimization to uncover the hidden temporal dynamics while aligning with LLMs sequential modeling abilities.

4.2. Multi-patch Prediction Fine-tuning

In this section, we fine-tune for the self-supervised, multi-patch prediction task, further refining patch representations to align with the target time series temporal contexts based on the casual next-patch pre-training model in Sec. 4.1.

Forward Process. As illustrated in Fig. 2 (b), given the i-th univariate time series $\boldsymbol{x}^{(i)}_{t:t+L-1} = \{x^{(i)}_t, ..., x^{(i)}_{t+L-1}\} \in \mathbb{R}^{1 \times L}$ of look-back window size L starting at time index t, the prediction horizon H and the time-series-aligned LLM $f_\theta(\cdot)$ trained in Sec. 4.1, we firstly prepare prediction anchors $\dot{\boldsymbol{x}}^{(i)}_{t+L:t+L+H-1} = \{\dot{x}^{(i)}_{t+L}, ..., \dot{x}^{(i)}_{t+L+H-1}\} \in \mathbb{R}^{1 \times H}$ through non-parametric methods (Recent history $\boldsymbol{x}^{(i)}_{t+L-H:t+L-1}$or Discrete fourier prediction). Then the look-back window input and anchors are divided into patch sequence $\boldsymbol{p}^{(i)}_{t_p:t_p+L_p-1} = \{\boldsymbol{p}^{(i)}_{t_p}, ..., \boldsymbol{p}^{(i)}_{t_p+L_p-1}\} \in \mathbb{R}^{L_p \times P}$ and $\dot{\boldsymbol{p}}^{(i)}_{t_p+L_p:t_p+L_p+H_p-1} = \{\dot{\boldsymbol{p}}^{(i)}_{t_p+L_p}, ..., \dot{\boldsymbol{p}}^{(i)}_{t_p+L_p+H_p-1}\} \in \mathbb{R}^{H_p \times P}$ where $t_p = \lfloor \frac{(t-P)}{S} \rfloor + 1$, $L_p = \lfloor \frac{(L-P)}{S} \rfloor + 1$, $H_p = \lfloor \frac{(H-P)}{S} \rfloor + 1$, P is the patch length, and S is the sliding stride. Next, these two patch sequences are concatenated and fed into the time-series-aligned LLM backbone $f_\theta(\cdot)$ trained in stage 1 with a position-aware attention mask $\mathbf{A}_p$, which enhances the temporal relationships among patches (Each future anchor can only see all accurate history patches and itself.). Finally, we employ the patch-wise projection layer $\mathbf{W}_p \in \mathbb{R}^{D \times P}$ to independently decode optimized anchors $\dot{\boldsymbol{p}}^{(i)_o}_{t_p+L_p:t_p+L_p+H_p-1} \in \mathbb{R}^{H_p \times D}$ into temporal patches $\hat{\boldsymbol{p}}^{(i)}_{t_p+L_p:t_p+L_p+H_p-1} \in \mathbb{R}^{H_p \times P}$, formulated as $\hat{\boldsymbol{p}}^{(i)}_{t_p+L_p+k} = \dot{\boldsymbol{p}}^{(i)_o}_{t_p+L_p+k} \mathbf{W}_p, k \in [0, H_p - 1]$.

Loss Function. We flatten the predicted patches from $\hat{\boldsymbol{p}}^{(i)}_{t_p+L_p:t_p+L_p+H_p-1}$ to $\hat{\boldsymbol{x}}^{(i)}_{t+L:t+L+H-1}$, gather and average the loss in M time series: $\mathcal{L}_s = \mathbb{E}_{\boldsymbol{x}} \frac{1}{M} \sum_{i=1}^{M} \|\hat{\boldsymbol{x}}^{(i)}_{t+L:t+L+H-1} - \boldsymbol{x}^{(i)}_{t+L:t+L+H-1}\|_2^2$. Notably, during multi-patch (anchor) representation optimization, most parameters in the time-series-aligned LLM $f_\theta(\cdot)$ trained in Sec. 4.1 are frozen except for the Position Embedding and Layer Normalization Layer (Less than 0.01% of the overall parameters) to make better adaptions in target time series. Also, once finish a single stage 2 adaption in a target time series dataset, history L, horizon H, we can perform any other forecasting tasks with other input/out length $\hat{L}/\hat{H}$ without any re-training since our patch-wise representation decoding is independent of input/out length.

5. Experiments

aLLM4TS consistently outperforms state-of-the-art time series analysis methods (Sec. 5.1) across multiple benchmarks and task settings, including long-term and short-term forecasting (Sec. 5.2 and Sec. 5.3), few-shot forecasting (Sec. 5.4), and anomaly detection (Sec. 5.5). We compared aLLM4TS against a broad collection of models, including the state-of-the-art LLM-based time series analysis model GPT4TS (Zhou et al., 2023).[3] Notably, in forecasting, based on our patch-wise decoder, aLLM4TS excels at handling arbitrary look-back window sizes and prediction horizons **with only one uniform training setting**, whereas previous methods necessitate re-training for each setting. Then, we provide additional analysis of representation learning ability and ablation study in Sec. 5.6 and Sec. 5.7. Due to the page limit, more experiment results are in the appendix, including imputation, classification, and other exploration experiments. We use the same default LLM backbone GPT-2 with the first 6 layers as GPT4TS (Zhou et al., 2023).

5.1. Experimental Settings

Datasets. For long-term forecasting, few-shot forecasting, and representation learning, we evaluate our proposed aLLM4TS on 8 popular datasets, including Weather, Traffic, Electricity, ILI, and 4 ETT datasets (ETTh1, ETTh2, ETTm1, ETTm2). These datasets have been extensively used and are publicly available in Wu et al. (2021). For short-term forecasting, we evaluate models on widely used marketing dataset M4 (Makridakis et al., 2018). For anomaly detection, we evaluate models on five widely employed datasets: SMD (Su et al., 2019), MSL (Hundman et al., 2018), SMAP (Hundman et al., 2018), SWaT (Mathur & Tippenhauer, 2016), and PSM (Abdulaal et al., 2021).

Baselines. For time series forecasting and anomaly de-

[3]To ensure fair comparisons, all experimental configurations are the same as Zhou et al. (2023) and follow a unified evaluation pipeline: `https://github.com/thuml/Time-Series-Library`. For current LLM-based methods (GPT4TS (Zhou et al., 2023) and Time-LLM (Jin et al., 2024)) that are not included in the pipeline, we reproduced their results through their official publicly available code (`https://github.com/DAMO-DI-ML/NeurIPS2023-One-Fits-All` and `https://github.com/KimMeen/Time-LLM`). Notably, we use GPT-2 (Radford et al., 2019) as the default backbone for all LLM-based methods.

Table 1: **Long-term Forecasting Results.** We calculate the MSE for each dataset. A lower value indicates better performance. **Red**: the best, Underlined: the second best. Due to the page limit, we put the full table in the appendix.

Methods		aLLM4TS	GPT4TS	Time-LLM	DLinear	PatchTST	TimesNet	FEDformer	Autoformer	Stationary	ETSformer	LightTS	Informer	Reformer
ETTh1	96	0.380	0.376	0.399	**0.375**	**0.375**	0.384	0.376	0.449	0.513	0.494	0.424	0.865	0.837
	192	**0.396**	0.416	0.433	0.405	0.414	0.436	0.420	0.500	0.534	0.538	0.475	1.008	0.923
	336	**0.413**	0.442	0.469	0.439	0.431	0.491	0.459	0.521	0.588	0.574	0.518	1.107	1.097
	720	0.461	0.477	0.473	0.472	**0.449**	0.521	0.506	0.514	0.643	0.562	0.547	1.181	1.257
ETTh2	96	**0.251**	0.285	0.294	0.289	0.274	0.340	0.358	0.346	0.476	0.340	0.397	3.755	2.626
	192	**0.298**	0.354	0.355	0.383	0.339	0.402	0.429	0.456	0.512	0.430	0.520	5.602	11.12
	336	0.343	0.373	0.372	0.448	**0.331**	0.452	0.496	0.482	0.552	0.485	0.626	4.721	9.323
	720	0.417	0.406	0.428	0.605	**0.379**	0.462	0.463	0.515	0.562	0.500	0.863	3.647	3.874
ILI	24	**1.359**	2.063	1.617	2.215	1.522	2.317	3.228	3.483	2.294	2.527	8.313	5.764	4.400
	36	**1.405**	1.868	1.708	1.963	1.430	1.972	2.679	3.103	1.825	2.615	6.631	4.755	4.783
	48	**1.442**	1.790	1.633	2.130	1.673	2.238	2.622	2.669	2.010	2.359	7.299	4.763	4.832
	60	1.603	1.979	2.106	2.368	**1.529**	2.027	2.857	2.770	2.178	2.487	7.283	5.264	4.882
Weather	96	**0.149**	0.162	0.163	0.176	0.152	0.172	0.217	0.266	0.173	0.197	0.182	0.300	0.689
	192	**0.190**	0.204	0.206	0.220	0.197	0.219	0.276	0.307	0.245	0.237	0.227	0.598	0.752
	336	**0.238**	0.254	0.255	0.265	0.249	0.280	0.339	0.359	0.321	0.298	0.282	0.578	0.639
	720	**0.316**	0.326	0.325	0.333	0.320	0.365	0.403	0.419	0.414	0.352	0.352	1.059	1.130
Traffic	96	0.372	0.388	0.383	0.410	**0.367**	0.593	0.587	0.613	0.612	0.607	0.615	0.719	0.732
	192	**0.383**	0.407	0.398	0.423	0.385	0.617	0.604	0.616	0.613	0.621	0.601	0.696	0.733
	336	**0.396**	0.412	0.407	0.436	0.398	0.629	0.621	0.622	0.618	0.622	0.613	0.777	0.742
	720	**0.433**	0.450	0.434	0.466	0.434	0.640	0.626	0.660	0.653	0.632	0.658	0.864	0.755
Electricity	96	**0.127**	0.139	0.140	0.140	0.130	0.168	0.193	0.201	0.169	0.187	0.207	0.274	0.312
	192	**0.145**	0.153	0.151	0.153	0.148	0.184	0.201	0.222	0.182	0.199	0.213	0.296	0.348
	336	**0.163**	0.169	0.171	0.169	0.167	0.198	0.214	0.231	0.200	0.212	0.230	0.300	0.350
	720	0.206	0.206	0.210	0.203	**0.202**	0.220	0.246	0.254	0.222	0.233	0.265	0.373	0.340

Table 2: **Short-term Forecasting Results.** We calculate the SMAPE for each dataset. A lower value indicates better performance. **Red**: the best. IMP. denotes the absolute SMAPE reduction of aLLM4TS compared with SOTA PLM-based GPT4TS, where a larger value indicates a better improvement. Due to the page limit, we put the full table in the appendix.

Methods	IMP.	aLLM4TS	GPT4TS	TimesNet	PatchTST	N-HiTS	N-BEATS	ETSformer	LightTS	DLinear	FEDformer	Stationary	Autoformer	Informer	Reformer
Yearly	**1.264**	13.540	14.804	**13.387**	13.477	13.418	13.436	18.009	14.247	16.965	13.728	13.717	13.974	14.727	16.169
Quarterly	**0.292**	10.216	10.508	**10.100**	10.38	10.202	10.124	13.376	11.364	12.145	10.792	10.958	11.338	11.360	13.313
Monthly	**0.206**	12.775	12.981	**12.670**	12.959	12.791	12.677	14.588	14.014	13.514	14.260	13.917	13.958	14.062	20.128
Others	**0.250**	5.032	5.282	**4.891**	4.952	5.061	4.925	7.267	15.880	6.709	4.954	6.302	5.485	24.460	32.491
Average	**0.472**	11.950	12.422	**11.829**	12.059	11.927	11.851	14.718	13.525	13.639	12.840	12.780	12.909	14.086	18.200

tection task, we compare 11 baseline methods: the SOTA LLM-based model GPT4TS (Zhou et al., 2023), nine Transformer-based models, including PatchTST (Nie et al., 2023), FEDformer (Zhou et al., 2022), Autoformer (Wu et al., 2021), Non-Stationary Transformer (Liu et al., 2022b), ESTformer (Woo et al., 2022b), LightTS (Zhang et al., 2022a), Pyraformer (Liu et al., 2021), Reformer (Kitaev et al., 2020), Informer (Zhou et al., 2021), and the SOTA MLP-based model DLinear (Zeng et al., 2023). And we also add a strong text-guided LLM baseline Time-LLM (Jin et al., 2024) for long-term forecasting. Besides, N-HiTS (Challu et al., 2022) and N-BEATS (Oreshkin et al., 2019) are added for comprehensive short-term forecasting performance comparison. For representation learning, we compare aLLM4TS with 5 baseline methods: the SOTA masking-based representation learning method PatchTST (Nie et al., 2023), and four contrastive learning methods for time series, BTSF (Yang & Hong, 2022), TS2Vec (Yue et al., 2022), TNC (Tonekaboni et al., 2021), and TS-TCC (Eldele et al., 2021).

Experiment Settings. For the time series forecasting task, all models follow the same experimental setup with prediction length $H \in \{24, 36, 48, 60\}$ for the ILI dataset and $H \in \{96, 192, 336, 720\}$ for other datasets. We use the default look-back window $L = 336$ for all baseline models and our proposed framework aLLM4TS.

Metrics. We use the following metrics in the experiment comparison: Mean Square Error (MSE), Mean Absolute Error (MAE), Symmetric Mean Absolute Percentage Error (SMAPE), and F1-score (Grishman & Sundheim, 1996).

5.2. Long-Term Time Series Forecasting

As shown in the table 1, aLLM4TS outperforms all baseline methods in most cases. Specifically, our informative two-stage forecasting-based, self-supervised representation optimization for LLMs and patch-wise decoding lead to an average performance improvement of $\mathbf{9.71\%}$ over GPT4TS, the current SOTA LLM-based method which directly employs

Table 3: **Few-shot Forecasting on** 5% **Data.** We calculate the MSE and MAE for each dataset. All results are averaged from 4 prediction lengths (96, 192, 336, and 720). **Red**: the best, Underlined: the second best. Due to the page limit, we put the full table in the appendix.

Methods	aLLM4TS		GPT4TS		DLinear		PatchTST		TimesNet		FEDformer		Autoformer		Stationary		ETSformer		LightTS		Informer		Reformer	
	MSE	MAE	MSE	MAE	MSE	MAE	MSE	MAE	MSE	MAE	MSE	MAE	MSE	MAE	MSE	MAE	MSE	MAE	MSE	MAE	MSE	MAE	MSE	MAE
ETTh1	**0.608**	**0.507**	0.681	0.560	0.750	0.611	0.694	0.569	0.925	0.647	0.658	0.562	0.722	0.598	0.943	0.646	1.189	0.839	1.451	0.903	1.225	0.817	1.241	0.835
ETTh2	**0.374**	**0.417**	0.400	0.433	0.694	0.577	0.827	0.615	0.439	0.448	0.463	0.454	0.441	0.457	0.470	0.489	0.809	0.681	3.206	1.268	3.922	1.653	3.527	1.472
ETTm1	0.419	**0.414**	0.472	0.450	**0.400**	0.417	0.526	0.476	0.717	0.561	0.730	0.592	0.796	0.620	0.857	0.598	1.125	0.782	1.123	0.765	1.163	0.791	1.264	0.826
ETTm2	**0.297**	**0.345**	0.308	0.346	0.399	0.426	0.314	0.352	0.344	0.372	0.381	0.404	0.388	0.433	0.341	0.372	0.534	0.547	1.415	0.871	3.658	1.489	3.581	1.487
Average	**0.425**	**0.421**	0.465	0.447	0.594	0.517	0.493	0.461	0.612	0.509	0.553	0.504	0.594	0.535	0.653	0.518	0.914	0.712	1.799	0.952	2.492	1.188	2.403	1.155

Table 4: **Anomaly Detection Results.** We calculate the F1-score (as %) for each dataset. **Red**: the best, Underlined: second best. $*$. in the Transformers indicates the name of $*$former. Due to the page limit, we put the full table in the appendix.

Methods	aLLM4TS Ours	GPT4TS	TimesNet	PatchTS.	ETS.	FED.	LightTS	DLinear	Stationary	Auto.	Pyra.	In.	Re.	LogTrans.	Trans.
SMD	85.42	**86.89**	84.61	84.62	83.13	85.08	82.53	77.10	84.72	85.11	83.04	81.65	75.32	76.21	79.56
MSL	82.26	82.45	81.84	78.70	**85.03**	78.57	78.95	84.88	77.50	79.05	84.86	84.06	84.40	79.57	78.68
SMAP	**78.04**	72.88	69.39	68.82	69.50	70.76	69.21	69.26	71.09	71.12	71.09	69.92	70.40	69.97	69.70
SWaT	**94.57**	94.23	93.02	85.72	84.91	93.19	93.33	87.52	79.88	92.74	91.78	81.43	82.80	80.52	80.37
PSM	97.19	97.13	**97.34**	96.08	91.76	97.23	97.15	93.55	97.29	93.29	82.08	77.10	73.61	76.74	76.07
Average	**87.51**	86.72	85.24	82.79	82.87	84.97	84.23	82.46	82.08	84.26	82.57	78.83	77.31	76.60	76.88

the sequence modeling capabilities in LLMs without any representation adaption. Compared to Time-LLM, which combines textual prompts with the sequence modeling capabilities of frozen LLMs, aLLM4TS achieves over $\mathbf{9.40\%}$ performance improvement. Compared with the SOTA Transformer model PatchTST, aLLM4TS realizes an average MSE reduction of 2.03%. Our improvements are also noteworthy compared with the other model classes, e.g., DLinear or TimesNet, exceeding $\mathbf{19.3\%}$. Notably, in stage 1, we conduct a shared casual next-patch pre-training with training sets of Weather, Traffic, Electricity, ILI, and 4 ETT datasets. In stage 2, for 4 horizons $H \in \{96, 192, 336, 720\}$ in a target dataset, aLLM4TS performs **only one** training for $H = 720$, then it can forecast arbitrary horizons due to its patch-wise decoder that is independent with horizon, while other baselines have to fine-tune for each horizon length.

5.3. Short-Term Time Series Forecasting

Table 2 shows the results of short-term forecasting in the M4 benchmark, which contains marketing data in different frequencies. Specifically, we use the same backbone as Sec. 5.2 which undergoes a casual next-patch pre-training on training sets of Weather, Traffic, Electricity, ILI, and 4 ETT datasets. Then we employ the same model configuration as GPT4TS to fine-tune for each frequency. We achieve a competitive performance close to the current SOTA TimesNet, whose CNN-based structure is usually considered to perform better in datasets characterized by diverse variations but limited volume (Wu et al., 2022), such as M4. The overall **0.472** SMAPE reduction compared with SOTA LLM-based GPT4TS is attributed to the importance of syncing LLM capabilities with the temporal dynamics. This also verifies the excellent transferability of our forecasting-aligned representation across time series from different domains.

5.4. Few-shot Time Series Forecasting

LLMs have demonstrated remarkable performance in few-shot learning (Liu et al., 2023; Brown et al., 2020) due to their ability to obtain strong general representations. In this section, we evaluate the few-shot forecasting ability of our time-series-aligned LLM in ETT datasets. To avoid data leakage, we conduct stage 1 on ETT1 datasets and perform multi-patch prediction with only **5**% training data in ETT2, and vice versa. The few-shot forecasting results are shown in Tab. 3. aLLM4TS remarkably excels over all baseline methods, and we attribute this to the successful representation syncing in our two-stage representation adaption. Notably, both our aLLM4TS and GPT4TS consistently outperform other competitive baselines, further verifying the potential of LLMs as effective time series machines. Significantly, aLLM4TS achieves an average MSE reduction of **8.6**% compared to SOTA LLM-based GPT4TS, indicating the benefits of our forecasting-based adaption and patch-wise decoding. In comparison to convolution-based TimesNet and MLP-based DLinear models that are usually considered more data-efficient for training and suitable for few-shot learning methods, aLLM4TS still demonstrates an average MSE reduction of **30.6**% and **28.5**% respectively.

5.5. Time Series Anomaly Detection

Time series anomaly detection has various industrial applications, such as health monitoring or finance evaluation. Similar to short-term forecasting, we use the same backbone as Sec. 5.2 which undergoes a casual next-patch pre-training on training sets of Weather, Traffic, Electricity, ILI, and 4 ETT datasets. Then we employ the same model configuration as GPT4TS to fine-tune in each anomaly dataset. Results in Tab. 4 demonstrate that aLLM4TS achieves the

Table 5: **Representation Learning Methods Comparison.** Sta_1 implies conducting stage 1, casual continual pre-training based on next-patch prediction in diverse time series. Sta_2 implies conducting stage 2, multi-patch prediction fine-tuning for target time series. Masking $- *\%$ implies replacing the origin stage 1 with masking-patch pre-training of masking ratio $**\%$ (*Masking* in PatchTST denotes using default masking ratio 40% as its origin paper). *SD* denotes replacing the patch-wise decoder in stage 2 with sequence-wise decoder. **Red**: the best, <u>Underlined</u>: the second best. IMP. denotes the improvement on best results of aLLM4TS compared to that of baselines.

Models		IMP.	aLLM4TS						PatchTST						BTSF		TS2Vec		TNC		TS-TCC	
			Sta_1+Sta_2		Masking-20%+Sta_2		Masking-40%+Sta_2		Sta_1+Sta_2		Masking+SD		Masking+Sta_2									
Metrics		MSE	MSE	MAE	MSE	MAE	MSE	MAE	MSE	MAE	MSE	MAE	MSE	MAE	MSE	MAE	MSE	MAE	MSE	MAE	MSE	MAE
ETTh1	24	6.52%	**0.301**	**0.362**	0.417	0.435	0.441	0.447	0.402	0.433	<u>0.322</u>	<u>0.369</u>	0.431	0.453	0.541	0.519	0.599	0.534	0.632	0.596	0.653	0.610
	48	3.48%	**0.343**	**0.377**	0.418	0.437	0.422	0.439	0.401	0.432	<u>0.354</u>	<u>0.385</u>	0.437	0.467	0.613	0.524	0.629	0.555	0.705	0.688	0.720	0.693
	168	6.21%	**0.393**	**0.415**	0.436	0.448	0.437	0.449	<u>0.416</u>	0.441	0.419	<u>0.424</u>	0.459	0.480	0.640	0.532	0.755	0.636	1.097	0.993	1.129	1.044
	336	7.20%	**0.413**	**0.428**	0.439	0.456	0.439	0.463	<u>0.440</u>	0.486	0.445	<u>0.446</u>	0.479	0.483	0.864	0.689	0.907	0.717	1.454	0.919	1.492	1.076
	720	5.34%	**0.461**	**0.462**	0.475	0.485	0.479	0.499	0.500	0.517	<u>0.487</u>	<u>0.478</u>	0.523	0.508	0.993	0.712	1.048	0.790	1.604	1.118	1.603	1.206

SOTA performance with the averaged F1-score **87.51**%. We attribute this better capability of detecting infrequent anomalies within time series to the forecasting-aligned representation learned in stage 1 casual next-patch pre-training on diverse time series. The aligning process syncs the LLM sequence modeling abilities with time series and further enhances the representation's transferability and generality across various time series domains and downstream tasks.

5.6. Representation Learning

In addition to aLLM4TS's outstanding performance across various downstream tasks, we further explore its superiority in adapting LLMs for time-series representation learning in ETTh1 forecasting. This is achieved through comparisons with state-of-the-art representation learning methods, and various comparative experiments for our two-stage forecasting-based aLLM4TS. Detailed results are in Tab. 5.

Sta_1: Casual Next-patch Pre-training. Comparing the column Sta_1+Sta_2 with column Masking+Sta_2[4], we observe a distinct average performance decline over **13.5**%, whether in a pre-trained LLM or a vanilla PatchTST. We attribute it to the challenge that masking-based patch pre-training struggles to model the vital temporal variations due to its random masking and reconstruction training paradigm. The results of other contrastive-learning-based methods also lead to a significant performance decline, as a result of the non-negligible non-alignment between their high-level objective with the downstream time series analysis tasks.

Sta_2: Multi-patch Prediction Fine-tuning. Previous patch-based models (Nie et al., 2023; Zhou et al., 2023) all choose to concatenate and project in sequence-level as in Fig. 1 ❷. Comparing column Masking+SD and Masking+Sta_2, more than **13.4**% deterioration occurs, strongly indicating the great risks of overfitting in the huge sequence-wise decoder.

5.7. Ablation Study

In this section, we conduct several ablations on framework design and the effectiveness of our two-stage forecasting-based self-supervised training. Brief results are in Tab. 6.

[4]Explanation of column names can be found in table caption.

[5]The $*(x)$ denotes using the first x layers of model $*$.

Table 6: **Ablations on ETT Dataset** (average MSE in prediction length $[96, 192, 336, 720]$ reported). **Red**: the best. Due to the page limit, we put the full table and analysis in the appendix.

Model Variant	Long-term Forecasting			
	ETTh1	ETTh2	ETTm1	ETTm2
A.1 aLLM4TS (**Default**: 6)[5]	**0.413**	**0.327**	**0.332**	0.294
A.2 aLLM4TS (3)	0.437	0.330	0.350	0.292
A.3 aLLM4TS (9)	0.452	0.339	0.404	0.307
A.4 aLLM4TS (12)	0.580	0.334	0.403	0.303
B.1 w/o Casual Continual Pre-training	0.460	0.350	0.373	0.307
B.2 w/o LLM Pretrained Weights (6)	0.437	0.336	0.364	0.301
B.3 w/o LLM Pretrained Weights (3)	0.462	0.339	0.373	0.305
C.1 w/o Patch-level Decoder	0.455	0.387	0.362	**0.284**
C.2 w/o Position-aware Attention Mask	0.443	0.358	0.399	0.303
D.1 Init with FFT	0.416	0.355	0.375	0.301
D.2 Init with Random	0.447	0.351	0.365	0.309
E.1 LN+PE+Attn	0.442	0.346	0.363	0.319
E.2 LN+PE+Attn+FFN	0.465	0.348	0.358	0.302

Casual Next-Patch Continual Pre-training. Comparing row A.1 and B.1 in Tab. 6, an average MSE increase of **8.80**% is observed, indicating that ablating casual next-patch continual pre-training significantly harms the sequence pattern recognition and forecasting modeling of the LLM for effective time series analysis. We attribute it to the inadequate adaption to apply pre-trained LLMs in time series without alignment that fits the temporal dynamics, forecasting modeling, and the casual pre-training of LLMs.

LLM Pre-trained Weight. We designed two sets of ablation experiments with different model sizes to avoid the mismatch between training data and model parameter quantity. We discard the pre-trained weights of the LLMs and train from scratch the first 6 layers (**B.2**) and the first 3 layers (**B.3**) of GPT-2. Ablating the LLM pre-trained weights directly results in the loss of the learned sequential representation capabilities from massive sequential text data (Zhou et al., 2023; Gruver et al., 2024). Consequently, it becomes difficult to learn the temporal representation from scratch within the LLM architecture, leading to the degradation in performance of **5.15**% and **7.91**%, respectively.

Patch-level Decoder. In ablation experiment **C.1**, we employed the conventional sequence-level decoder, resulting in an average performance loss exceeding **8.54**%. Despite using a decoder over 100 times larger and can train specifically for each input/output length, a substantial performance loss occurred. This is attributed to the potential downstream task overfitting of the huge sequence-level head and the incapability to disentangle the patch representation encoding and decoding process, leading to inadequate patch representation optimization in the LLM backbone.

Position-aware Attention Mask. In aLLM4TS, we transform the forecasting into multi-patch representation optimization based on well-aligned patch-based time series knowledge. Position-aware attention mask is designed to further enhance the optimization process by removing the unwanted confusion brought by other being-optimized anchors during the optimization. Ablation of this component (**C.2**) results in over **10.01**% performance deterioration.

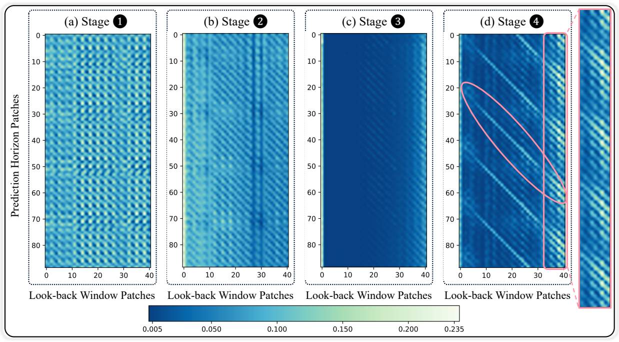

Figure 3: Interpretability study in Traffic dataset. Due to the page limit, we put the full visualization and analysis in the appendix. The Y-axis and X-axis represent prediction horizon patch indexes and look-back window patch indexes, respectively.

5.8. Interpretability Experiment

We conducted a case study on the Traffic dataset to illustrate the evolution of attention weights from the prediction horizon patches to look-back window patches at four stages in Fig. 3. The 4 subplots detail the attention weights optimization process from randomly-initialized (Stage ❶), through LLMs-pre-trained (Stage ❷), casually next-patch continual pre-trained (Stage ❸) to multi-patch prediction adaption (Stage ❹). Our observations are as follows: **Obs.①** **After stage ❹, aLLM4TS adeptly captures the complex multi-periodic properties of time series and a discernible trend of increasing information importance along the temporal dimension.** In Fig. 3 (d), look-back window patches closest to the prediction horizon exhibit similar patterns from prediction horizon patches at time steps t, $t+3$, $\cdots$. With a patch size of 16 and a stride of 8, sampling hourly, this corresponds to local day cycles. Additionally, there exist 20-patch cycles (equivalent to 168 hours), indicating weekly cycles. Furthermore, look-back window patches closer to the predicted horizon receive increasing attention due to their temporal proximity, indicating their greater informational significance. **Obs.② After stage ❸, aLLM4TS learns universal single-period features (e.g., day) and showcases a noticeable trend of increasing attention along the time dimension** in Fig. 3 (c), stemming from the process of casually predicting the next patch. **Obs.③ Pre-trained LLM parameters capture fundamental time-series cycle attributes** in Fig. 3 (a) and (b), serving as a robust optimization anchor for time-series representation learning when compared with random initialization.

6. Conclusion

In this paper, we introduce *aLLM4TS*, a novel framework that adapts Large Language Models (LLMs) for time-series representation learning. By reframing time-series forecasting as a self-supervised, multi-patch prediction task, our approach surpasses conventional mask-and-reconstruction techniques, more adeptly capturing the hidden temporal dynamics within patch representations. Notably, *aLLM4TS* introduces a patch-wise decoding mechanism, a departure from traditional sequence-wise decoding, allowing for the independent decoding of patches into temporal sequences. This significantly bolsters the LLM backbone's aptitude for temporal patch-based representation learning. *aLLM4TS* exhibits superior performance across various downstream tasks, substantiating its efficacy in deriving temporal representations with enhanced transferability, marking a pivotal stride in adapting LLMs for advanced time-series analysis.

Acknowledgements

This work is supported in part by the Research Matching Grant Scheme under Grant No. 8601440, in part by the National Natural Science Foundation of China (Grant no. 62102287), and in part by the Shanghai Science and Technology Innovation Action Plan Project (Grant no. 22YS1400600 and 22511100700).

Impact Statement

Our work on time series representation learning presents no immediate ethical concerns but carries the potential for misuse and socio-economic impacts. Misuse could involve unethical exploitation in various domains, while the socio-economic effects might include significant shifts in industries and labor markets. Addressing these concerns necessitates robust ethical guidelines and a thorough consideration of broader implications to ensure that the deployment of these models is fair, responsible, and beneficial to society.

References

Abdulaal, A., Liu, Z., and Lancewicki, T. Practical approach to asynchronous multivariate time series anomaly detection and localization. In *KDD*, 2021.

Bagnall, A., Dau, H. A., Lines, J., Flynn, M., Large, J., Bostrom, A., Southam, P., and Keogh, E. The uea multivariate time series classification archive, 2018. *arXiv:1811.00075*, 2018.

Borsos, Z., Marinier, R., Vincent, D., Kharitonov, E., Pietquin, O., Sharifi, M., Roblek, D., Teboul, O., Grangier, D., Tagliasacchi, M., et al. Audiolm: a language modeling approach to audio generation. *IEEE/ACM Transactions on Audio, Speech, and Language Processing*, 2023.

Box, G. E. and Jenkins, G. M. Some recent advances in forecasting and control. *Journal of the Royal Statistical Society. Series C (Applied Statistics)*, 1968.

Brown, T. B., Mann, B., Ryder, N., Subbiah, M., Kaplan, J., Dhariwal, P., Neelakantan, A., Shyam, P., Sastry, G., Askell, A., Agarwal, S., Herbert-Voss, A., Krueger, G., Henighan, T., Child, R., Ramesh, A., Ziegler, D. M., Wu, J., Winter, C., Hesse, C., Chen, M., Sigler, E., Litwin, M., Gray, S., Chess, B., Clark, J., Berner, C., McCandlish, S., Radford, A., Sutskever, I., and Amodei, D. Language models are few-shot learners. In *NeurIPS*, 2020.

Cao, D., Jia, F., Arik, S. O., Pfister, T., Zheng, Y., Ye, W., and Liu, Y. TEMPO: Prompt-based generative pre-trained transformer for time series forecasting. In *ICLR*, 2024.

Challu, C., Olivares, K. G., Oreshkin, B. N., Garza, F., Mergenthaler, M., and Dubrawski, A. N-hits: Neural hierarchical interpolation for time series forecasting. *CoRR*, abs/2201.12886, 2022.

Chang, C., Peng, W.-C., and Chen, T.-F. Llm4ts: Two-stage fine-tuning for time-series forecasting with pre-trained llms. *arXiv:2308.08469*, 2023.

Dempster, A., Petitjean, F., and Webb, G. I. Rocket: exceptionally fast and accurate time series classification using random convolutional kernels. *Data Mining and Knowledge Discovery*, 2020.

Dong, J., Wu, H., Zhang, H., Zhang, L., Wang, J., and Long, M. Simmtm: A simple pre-training framework for masked time-series modeling. *arXiv:2302.00861*, 2023.

Eldele, E., Ragab, M., Chen, Z., Wu, M., Kwoh, C. K., Li, X., and Guan, C. Time-series representation learning via temporal and contextual contrasting. In *IJCAI*, 2021.

Ethayarajh, K. How contextual are contextualized word representations? comparing the geometry of bert, elmo, and gpt-2 embeddings. *arXiv:1909.00512*, 2019.

Fortuin, V., Hüser, M., Locatello, F., Strathmann, H., and Rätsch, G. Deep self-organization: Interpretable discrete representation learning on time series. In *ICLR*, 2019.

Franceschi, J.-Y., Dieuleveut, A., and Jaggi, M. Unsupervised scalable representation learning for multivariate time series. *NeurIPS*, 2019.

Grishman, R. and Sundheim, B. M. Message understanding conference-6: A brief history. In *COLING 1996 Volume 1: The 16th International Conference on Computational Linguistics*, 1996.

Gruver, N., Finzi, M., Qiu, S., and Wilson, A. G. Large language models are zero-shot time series forecasters. In *NeurIPS*, 2024.

Gu, A., Goel, K., and Ré, C. Efficiently modeling long sequences with structured state spaces. *arXiv:2111.00396*, 2021.

Houlsby, N., Giurgiu, A., Jastrzebski, S., Morrone, B., De Laroussilhe, Q., Gesmundo, A., Attariyan, M., and Gelly, S. Parameter-efficient transfer learning for nlp. In *ICML*, 2019.

Hundman, K., Constantinou, V., Laporte, C., Colwell, I., and Soderstrom, T. Detecting spacecraft anomalies using lstms and nonparametric dynamic thresholding. In *KDD*, 2018.

Jin, M., Wang, S., Ma, L., Chu, Z., Zhang, J. Y., Shi, X., Chen, P.-Y., Liang, Y., Li, Y.-F., Pan, S., and Wen, Q. Time-LLM: Time series forecasting by reprogramming large language models. In *ICLR*, 2024.

Kitaev, N., Kaiser, L., and Levskaya, A. Reformer: The efficient transformer. In *ICLR*, 2020.

Lai, G., Chang, W.-C., Yang, Y., and Liu, H. Modeling long-and short-term temporal patterns with deep neural networks. In *SIGIR*, 2018.

Lee, S., Park, T., and Lee, K. Learning to embed time series patches independently. *arXiv:2312.16427*, 2023.

Li, Z., Rao, Z., Pan, L., Wang, P., and Xu, Z. Ti-mae: Self-supervised masked time series autoencoders. *arXiv:2301.08871*, 2023.

Liu, M., Zeng, A., Chen, M., Xu, Z., Lai, Q., Ma, L., and Xu, Q. Scinet: Time series modeling and forecasting with sample convolution and interaction. *NeurIPS*, 2022a.

Liu, S., Yu, H., Liao, C., Li, J., Lin, W., Liu, A. X., and Dustdar, S. Pyraformer: Low-complexity pyramidal attention for long-range time series modeling and forecasting. In *ICLR*, 2021.

Liu, X., McDuff, D., Kovacs, G., Galatzer-Levy, I., Sunshine, J., Zhan, J., Poh, M.-Z., Liao, S., Di Achille, P., and Patel, S. Large language models are few-shot health learners. *arXiv:2305.15525*, 2023.

Liu, Y., Wu, H., Wang, J., and Long, M. Non-stationary transformers: Exploring the stationarity in time series forecasting. In *NeurIPS*, 2022b.

Lu, K., Grover, A., Abbeel, P., and Mordatch, I. Frozen pretrained transformers as universal computation engines. *AAAI*, 2022.

Lu, S., Chen, L.-H., Zeng, A., Lin, J., Zhang, R., Zhang, L., and Shum, H.-Y. Humantomato: Text-aligned whole-body motion generation. *arXiv:2310.12978*, 2023.

Ma, Q., Liu, Z., Zheng, Z., Huang, Z., Zhu, S., Yu, Z., and Kwok, J. T. A survey on time-series pre-trained models. *arXiv:2305.10716*, 2023.

Makridakis, S., Spiliotis, E., and Assimakopoulos, V. The m4 competition: Results, findings, conclusion and way forward. *International Journal of Forecasting*, 2018.

Mathur, A. P. and Tippenhauer, N. O. Swat: A water treatment testbed for research and training on ics security. In *2016 international workshop on cyber-physical systems for smart water networks (CySWater)*, 2016.

Memory, L. S.-T. Long short-term memory. *Neural computation*, 2010.

Nie, Y., Nguyen, N. H., Sinthong, P., and Kalagnanam, J. A time series is worth 64 words: Long-term forecasting with transformers. In *ICLR*, 2023.

OpenAI. Chatgpt, 2023.

Oreshkin, B. N., Carpov, D., Chapados, N., and Bengio, Y. N-beats: Neural basis expansion analysis for interpretable time series forecasting. *arXiv:1905.10437*, 2019.

Radford, A., Wu, J., Child, R., Luan, D., Amodei, D., Sutskever, I., et al. Language models are unsupervised multitask learners. *OpenAI blog*, 2019.

Spathis, D. and Kawsar, F. The first step is the hardest: Pitfalls of representing and tokenizing temporal data for large language models. *arXiv:2309.06236*, 2023.

Su, Y., Zhao, Y., Niu, C., Liu, R., Sun, W., and Pei, D. Robust anomaly detection for multivariate time series through stochastic recurrent neural network. In *KDD*, 2019.

Sun, C., Li, H., Li, Y., and Hong, S. TEST: Text prototype aligned embedding to activate LLM's ability for time series. In *ICLR*, 2024.

Taylor, S. J. and Letham, B. Forecasting at scale. *The American Statistician*, 2018.

Tonekaboni, S., Eytan, D., and Goldenberg, A. Unsupervised representation learning for time series with temporal neighborhood coding. In *ICLR*, 2021.

Woo, G., Liu, C., Sahoo, D., Kumar, A., and Hoi, S. Cost: Contrastive learning of disentangled seasonal-trend representations for time series forecasting. *arXiv:2202.01575*, 2022a.

Woo, G., Liu, C., Sahoo, D., Kumar, A., and Hoi, S. Etsformer: Exponential smoothing transformers for time-series forecasting. *arXiv:2202.01381*, 2022b.

Wu, H., Xu, J., Wang, J., and Long, M. Autoformer: Decomposition transformers with auto-correlation for long-term series forecasting. In *NeurIPS*, 2021.

Wu, H., Hu, T., Liu, Y., Zhou, H., Wang, J., and Long, M. Timesnet: Temporal 2d-variation modeling for general time series analysis. In *ICLR*, 2022.

Xie, Z., Geng, Z., Hu, J., Zhang, Z., Hu, H., and Cao, Y. Revealing the dark secrets of masked image modeling. In *CVPR*, 2023.

Xu, J., Wu, H., Wang, J., and Long, M. Anomaly transformer: Time series anomaly detection with association discrepancy. In *ICLR*, 2021.

Xu, Z., Zeng, A., and Xu, Q. FITS: Modeling time series with \$10k\$ parameters. In *ICLR*, 2024.

Xue, H. and Salim, F. D. Promptcast: A new prompt-based learning paradigm for time series forecasting. *IEEE Transactions on Knowledge and Data Engineering*, 2023.

Yang, L. and Hong, S. Unsupervised time-series representation learning with iterative bilinear temporal-spectral fusion. In *ICML*, 2022.

Yu, X., Chen, Z., Ling, Y., Dong, S., Liu, Z., and Lu, Y. Temporal data meets llm–explainable financial time series forecasting. *arXiv:2306.11025*, 2023.

Yue, Z., Wang, Y., Duan, J., Yang, T., Huang, C., Tong, Y., and Xu, B. Ts2vec: Towards universal representation of time series. *AAAI*, 2022.

Zeng, A., Chen, M., Zhang, L., and Xu, Q. Are transformers effective for time series forecasting? *AAAI*, 2023.

Zerveas, G., Jayaraman, S., Patel, D., Bhamidipaty, A., and Eickhoff, C. A transformer-based framework for multivariate time series representation learning. In *KDD*, 2021.

Zhang, T., Zhang, Y., Cao, W., Bian, J., Yi, X., Zheng, S., and Li, J. Less is more: Fast multivariate time series forecasting with light sampling-oriented mlp structures. *arXiv:2207.01186*, 2022a.

Zhang, X., Zhao, Z., Tsiligkaridis, T., and Zitnik, M. Self-supervised contrastive pre-training for time series via time-frequency consistency. In *NeurIPS*, 2022b.

Zhou, H., Zhang, S., Peng, J., Zhang, S., Li, J., Xiong, H., and Zhang, W. Informer: Beyond efficient transformer for long sequence time-series forecasting. *AAAI*, 2021.

Zhou, T., Ma, Z., Wen, Q., Wang, X., Sun, L., and Jin, R. Fedformer: Frequency enhanced decomposed transformer for long-term series forecasting. In *ICML*, 2022.

Zhou, T., Niu, P., Sun, L., Jin, R., et al. One fits all: Power general time series analysis by pretrained lm. In *NeurIPS*, 2023.

A. Visualization

In this section, we present visualizations of the forecasting achieved by aLLM4TS in comparison to state-of-the-art and representative methods, including GPT4TS (Zhou et al., 2023), PatchTST (Nie et al., 2023), DLinear (Zeng et al., 2023), N-HITS (Challu et al., 2022), and TimesNet (Wu et al., 2022), for long-term and short-term forecasting. The accompanying figures (Fig. 4 and Fig. 5) illustrate the comparison between the long-term (input-96-predict-96) and short-term (input-96-predict-48) forecasts of various approaches against the ground truth. Notably, aLLM4TS exhibits superior forecasting accuracy when compared with the state-of-the-art LLM-based GPT4TS (Zhou et al., 2023), transformer-based PatchTST (Nie et al., 2023), MLP-based DLinear (Zeng et al., 2023), MLP-based N-HITS (Challu et al., 2022) and CNN-based TimesNet (Wu et al., 2022).

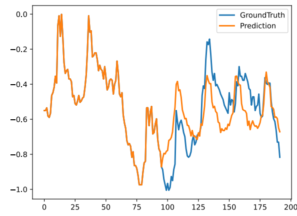

(a) aLLM4TS

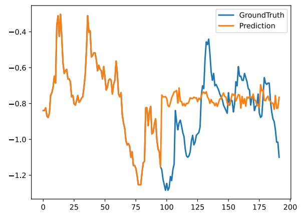

(b) GPT4TS

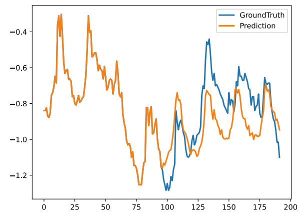

(c) PatchTST

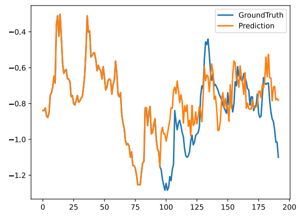

(d) Dlinear

Figure 4: Long-term forecasting cases from ETTh1 by different models under the input-96-predict-96 settings. Blue lines are the ground truths and orange lines are the model predictions.

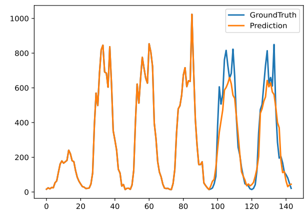

(a) aLLM4TS

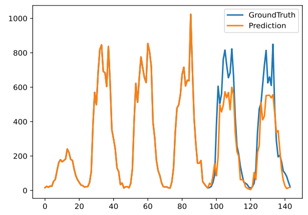

(b) GPT4TS

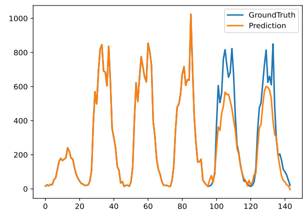

(c) TimesNet

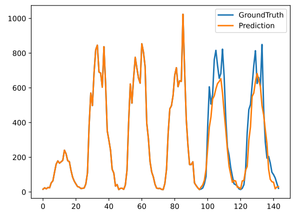

(d) N-HITS

Figure 5: Short-term forecasting from the M4 hourly dataset by different models under the input-96-predict-48 settings. Blue lines are the ground truths and orange lines are the model predictions.

B. More Related Work

B.1. Time Series Forecasting

Time series forecasting has undergone extensive exploration and study as a pivotal task. From early statistical methods (Box & Jenkins, 1968; Taylor & Letham, 2018) to recent deep learning approaches based on MLP (Zeng et al., 2023; Zhang et al., 2022a; Oreshkin et al., 2019; Challu et al., 2022), TCN(Franceschi et al., 2019) or RNN(Gu et al., 2021; Lai et al., 2018; Memory, 2010), researchers have been continuously modeling time series forecasting from various perspectives. Recently, transformers (Nie et al., 2023; Wu et al., 2021; Liu et al., 2021; Zhou et al., 2022) have demonstrated remarkable effectiveness in time series forecasting. Leveraging attention mechanisms, they excel in uncovering temporal dependencies among different time points and mining sequence representation. Notably, PatchTST (Nie et al., 2023) first proposes using patches as the fundamental processing unit for time series and explores the capabilities of patch-based representation learning within an self-supervised masking setting.

B.2. Time Series Representation Learning

Recently, there has been a growing focus on time series representation learning. Previous self-supervised learning methods can be roughly divided into two classes: (1) **Contrastive Learning.** These methods aim to optimize the representation space based on subseries consistency (Franceschi et al., 2019; Fortuin et al., 2019), temporal consistency (Tonekaboni et al., 2021;

Woo et al., 2022a; Yue et al., 2022), transformation consistency (Zhang et al., 2022b; Yang & Hong, 2022) or contextual consistency (Eldele et al., 2021), where representations of positive pairs are optimized to be close to each other and negative ones to be far apart. For instance, TS2Vec (Yue et al., 2022) splits multiple time series into patches and further defines the contrastive loss in both instance-wise and patch-wise aspects. TS-TCC (Eldele et al., 2021) optimizes the representation by making the augmentations predict each other's future. However, these methods suffer from poor alignment with low-level tasks, such as forecasting, due to the main focus on high-level information (Xie et al., 2023). (2) **Masked Modeling.** The fundamental insight behind masked modeling is to learn abstract representation by reconstructing the masked period from the unmasked content (Nie et al., 2023; Dong et al., 2023; Li et al., 2023). PatchTST (Nie et al., 2023) first proposes using patches as the fundamental processing unit for time series and explores predict masked subseries-level patches to capture the local semantic information and reduce memory usage. SimMTM (Dong et al., 2023) reconstructs the original time series from multiple randomly masked series. However, masking modeling not only disrupts temporal dependencies but also fails to ensure sufficient learning of temporal dynamics, as masked values are often easily reconstructed from the surrounding contexts (Li et al., 2023).

B.3. Time Series Analysis based on LLMs

Recently, many works have been trying to adapt pre-trained LLMs' excellent sequence representation learning ability in time series analysis. (1) **Zero-shot Adaption.** Gruver et al. (2024); Xue & Salim (2023); Yu et al. (2023) directly adapt the sequence representation ability of frozen LLMs for obtaining time series prediction. (2) **Prompt Optimization.** Jin et al. (2024); Cao et al. (2024); Sun et al. (2024) combine the reprogrammed input time series with the inherited sequence modeling ability within pre-trained LLMs to achieve future forecasting. (3) **Limited Finetuning.** Zhou et al. (2023); Liu et al. (2023); Chang et al. (2023) fine-tune specific parts of LLMs in target datasets for better time series analysis task performance. However, these methods end with relatively poor performance due to limited adapting strategies (Sun et al., 2024; Spathis & Kawsar, 2023), where a representation adaption pre-training and an appropriate patch-wise decoder are needed to transfer the sequential representation capabilities of LLM into time series analysis.

In this paper, we aim to fundamentally adapt LLMs for time series based on a two-stage forecasting-based self-supervised training strategy, including the casual next-patch pre-training and multi-patch prediction fine-tuning. Additionally, we devise a patch-wise decoding layer to disentangle the encoding and decoding process in patch-based time series modeling, boosting the LLM backbone to effectively focus on patch-based representation optimization. Our aLLM4TS stands as a novel framework in redefining the landscape of adapting LLMs into time series analysis.

C. Dataset Details

For forecasting and imputation, we utilize eight widely recognized multivariate datasets, as presented in Wu et al. (2021), and their specifics are outlined in Tab. 7. The *Weather*[6] dataset encompasses 21 meteorological indicators in Germany, while the *Traffic*[7] dataset records road occupancy rates from various sensors on San Francisco freeways. The *Electricity*[8] dataset comprises hourly electricity consumption data for 321 customers. The *ILI*[9] dataset captures the count of patients and the influenza-like illness ratio weekly. The *ETT*[10] (Electricity Transformer Temperature) datasets are sourced from two distinct electric transformers labeled 1 and 2, each featuring two resolutions (15 minutes and 1 hour) denoted as "m" and "h". Consequently, we have a total of four ETT datasets: *ETTm1*, *ETTm2*, *ETTh1*, and *ETTh2*.

Table 7: Statistics of Forecasting and Imputation Benchmark Datasets.

Datasets	Weather	Traffic	Electricity	ILI	ETTh1	ETTh2	ETTm1	ETTm2
Features	21	862	321	7	7	7	7	7
Timesteps	52696	17544	26304	966	17420	17420	69680	69680
Frequency	10 min	15 min	Hourly	Weekly	Hourly	Hourly	15 min	15 min

[6]https://www.bgc-jena.mpg.de/wetter/
[7]https://pems.dot.ca.gov/
[8]https://archive.ics.uci.edu/ml/datasets/ElectricityLoadDiagrams20112014
[9]https://gis.cdc.gov/grasp/fluview/fluportaldashboard.html
[10]https://github.com/zhouhaoyi/ETDataset

For anomaly detection, we evaluate models on five widely employed datasets: SMD (Su et al., 2019), MSL (Hundman et al., 2018), SMAP (Hundman et al., 2018), SWaT (Mathur & Tippenhauer, 2016), and PSM (Abdulaal et al., 2021).

1. The Server Machine Dataset (SMD, (Su et al., 2019)) spans five weeks and originates from a prominent Internet company, encompassing 38 dimensions.
2. Pooled Server Metrics (PSM, (Abdulaal et al., 2021)) are internally collected from various application server nodes at eBay, encompassing 26 dimensions.
3. Both the MSL (Mars Science Laboratory rover) and SMAP (Soil Moisture Active Passive satellite) datasets, publicly available from NASA (Hundman et al., 2018), consist of 55 and 25 dimensions, respectively. These datasets encompass telemetry anomaly information extracted from the Incident Surprise Anomaly (ISA) reports of spacecraft monitoring systems.
4. SWaT (Secure Water Treatment, (Mathur & Tippenhauer, 2016)), is derived from the data collected by 51 sensors within the critical infrastructure system operating continuously.

Table 8: Statistics of Anomaly Detection Benchmark Datasets (Xu et al., 2021). Abnormal Proportion represents the true abnormal proportion of the whole dataset.

Benchmarks	Applications	Dimension	Window	#Training	#Validation	#Test (labeled)	Abnormal Proportion
SMD	Server	38	100	566,724	141,681	708,420	0.042
PSM	Server	25	100	105,984	26,497	87,841	0.278
MSL	Space	55	100	46,653	11,664	73,729	0.105
SMAP	Space	25	100	108,146	27,037	427,617	0.128
SWaT	Water	51	100	396,000	99,000	449,919	0.121

D. Experimental Details

D.1. Implementation

We adopt the experimental setups introduced by Zhou et al. (2023) for all baseline models, ensuring a consistent evaluation pipeline accessible at `https://github.com/thuml/Time-Series-Library` to facilitate fair comparisons. GPT-2 (Radford et al., 2019), specifically its first 6 layers, is employed as the default backbone model unless explicitly specified. Our model is implemented in PyTorch, and all experiments are executed on NVIDIA A800-80G GPUs. Moreover, we enhance memory efficiency by transforming multivariate data into univariate data, treating each feature of the sequence as an individual time series. This aligns with the demonstrated efficacy of channel independence in prior works such as DLinear (Zeng et al., 2023) and PatchTST (Nie et al., 2023).

D.2. Evaluation Metrics

We utilize mean square error (MSE) and mean absolute error (MAE) for evaluating long-term forecasting, few-shot forecasting, and imputation. For short-term forecasting on the M4 benchmark, we employ the symmetric mean absolute percentage error (SMAPE), mean absolute scaled error (MASE), and overall weighted average (OWA) following the approach in N-BEATS (Oreshkin et al., 2019), where OWA is a metric specific to the M4 competition. Anomaly detection employs Precision, Recall, and F1-score, with the metric calculations outlined as follows:

$$\text{MSE} = \frac{1}{H}\sum_{h=1}^{T}(\mathbf{Y}_h - \hat{\mathbf{Y}}_h)^2, \qquad \text{MAE} = \frac{1}{H}\sum_{h=1}^{H}|\mathbf{Y}_h - \hat{\mathbf{Y}}_h|, \tag{4}$$

$$\text{SMAPE} = \frac{200}{H}\sum_{h=1}^{H}\frac{|\mathbf{Y}_h - \hat{\mathbf{Y}}_h|}{|\mathbf{Y}_h| + |\hat{\mathbf{Y}}_h|}, \qquad \text{MAPE} = \frac{100}{H}\sum_{h=1}^{H}\frac{|\mathbf{Y}_h - \hat{\mathbf{Y}}_h|}{|\mathbf{Y}_h|}, \tag{5}$$

$$\text{MASE} = \frac{1}{H}\sum_{h=1}^{H}\frac{|\mathbf{Y}_h - \hat{\mathbf{Y}}_h|}{\frac{1}{H-s}\sum_{j=s+1}^{H}|\mathbf{Y}_j - \mathbf{Y}_{j-s}|}, \qquad \text{OWA} = \frac{1}{2}\left[\frac{\text{SMAPE}}{\text{SMAPE}_{\text{Naïve2}}} + \frac{\text{MASE}}{\text{MASE}_{\text{Naïve2}}}\right], \tag{6}$$

$$\text{Precision} = \frac{\hat{\mathbf{N}}_{TP}}{\hat{\mathbf{N}}_{TP} + \hat{\mathbf{N}}_{FP}} \qquad \text{Recall} = \frac{\hat{\mathbf{N}}_{TP}}{\hat{\mathbf{N}}_{TP} + \hat{\mathbf{N}}_{FN}}. \tag{7}$$

H denotes the number of data points, signifying the prediction horizon in our experiments. s denotes the periodicity of the time series data. $\mathbf{Y}_h$ and $\hat{\mathbf{Y}}_h$ correspond to the h-th ground truth and prediction where $h \in \{1, \cdots, H\}$. $\hat{\mathbf{N}}_{TP}$ is the number of true positives in prediction, $\hat{\mathbf{N}}_{FP}$ is the number of false positives in prediction, $\hat{\mathbf{N}}_{FN}$ is the number of true negatives in prediction, F1-score $= \frac{2 \cdot \text{Precision} \cdot \text{Recall}}{\text{Precision} + \text{Recall}}$.

D.3. Detailed Definition and Results for Few-shot and Long-term Forecasting

Given the validated efficacy of channel independence in time series datasets by Zeng et al. (2023) and Nie et al. (2023), we opt for an approach wherein each multivariate series is treated as a distinct independent univariate series. Following standard experimental protocols, we partition each time series into training, validation, and test sets. Specifically, for the few-shot forecasting task, only a designated percentage (5%) of timesteps from the training data are used, while the remaining two parts remain unchanged. The assessment metrics align with those employed in classic multivariate time series forecasting. This experiment is conducted thrice, and the subsequent analyses report the average metrics. Detailed results for few-shot time-series forecasting are presented in Table 10.

Table 9: **Full Long-term Forecasting Results.** We use forecasting horizons $H \in \{96, 192, 336, 720\}$. We calculate the MSE for each dataset. A lower value indicates better performance. **Red**: the best, Underlined: the second best.

Methods		aLLM4TS	GPT4TS	Time-LLM	DLinear	PatchTST	TimesNet	FEDformer	Autoformer	Stationary	ETSformer	LightTS	Informer	Reformer
Weather	96	**0.149**	0.162	0.163	0.176	0.152	0.172	0.217	0.266	0.173	0.197	0.182	0.300	0.689
	192	**0.190**	0.204	0.206	0.220	0.197	0.219	0.276	0.307	0.245	0.237	0.227	0.598	0.752
	336	**0.238**	0.254	0.255	0.265	0.249	0.280	0.339	0.359	0.321	0.298	0.282	0.578	0.639
	720	**0.316**	0.326	0.325	0.333	0.320	0.365	0.403	0.419	0.414	0.352	0.352	1.059	1.130
Traffic	96	0.372	0.388	0.383	0.410	**0.367**	0.593	0.587	0.613	0.612	0.607	0.615	0.719	0.732
	192	**0.383**	0.407	0.398	0.423	0.385	0.617	0.604	0.616	0.613	0.621	0.601	0.696	0.733
	336	**0.396**	0.412	0.407	0.436	0.398	0.629	0.621	0.622	0.618	0.622	0.613	0.777	0.742
	720	**0.434**	0.450	0.434	0.466	0.434	0.640	0.626	0.660	0.653	0.632	0.658	0.864	0.755
Electricity	96	**0.127**	0.139	0.140	0.140	0.130	0.168	0.193	0.201	0.169	0.187	0.207	0.274	0.312
	192	**0.145**	0.153	0.151	0.153	0.148	0.184	0.201	0.222	0.182	0.199	0.213	0.296	0.348
	336	**0.163**	0.169	0.171	0.169	0.167	0.198	0.214	0.231	0.200	0.212	0.230	0.300	0.350
	720	0.206	0.206	0.210	0.203	**0.202**	0.220	0.246	0.254	0.222	0.233	0.265	0.373	0.340
ETTh1	96	0.380	0.376	0.399	**0.375**	**0.375**	0.384	0.376	0.449	0.513	0.494	0.424	0.865	0.837
	192	**0.396**	0.416	0.433	0.405	0.414	0.436	0.420	0.500	0.534	0.538	0.475	1.008	0.923
	336	**0.413**	0.442	0.469	0.439	0.431	0.491	0.459	0.521	0.588	0.574	0.518	1.107	1.097
	720	0.461	0.477	0.473	0.472	**0.449**	0.521	0.506	0.514	0.643	0.562	0.547	1.181	1.257
ETTh2	96	**0.251**	0.285	0.294	0.289	0.274	0.340	0.358	0.346	0.476	0.340	0.397	3.755	2.626
	192	**0.298**	0.354	0.355	0.383	0.339	0.402	0.429	0.456	0.512	0.430	0.520	5.602	11.12
	336	0.343	0.373	0.372	0.448	**0.331**	0.452	0.496	0.482	0.552	0.485	0.626	4.721	9.323
	720	0.417	0.406	0.428	0.605	**0.379**	0.462	0.463	0.515	0.562	0.500	0.863	3.647	3.874
ETTm1	96	**0.290**	0.292	0.293	0.299	0.290	0.338	0.379	0.505	0.386	0.375	0.374	0.672	0.538
	192	**0.316**	0.332	0.333	0.335	0.332	0.374	0.426	0.553	0.459	0.408	0.400	0.795	0.658
	336	**0.342**	0.366	0.367	0.369	0.366	0.410	0.445	0.621	0.495	0.435	0.438	1.212	0.898
	720	**0.381**	0.417	0.435	0.425	0.420	0.478	0.543	0.671	0.585	0.499	0.527	1.166	1.102
ETTm2	96	0.171	0.173	0.178	0.167	**0.165**	0.187	0.203	0.255	0.192	0.189	0.209	0.365	0.658
	192	0.234	0.229	0.245	0.224	**0.220**	0.249	0.269	0.281	0.280	0.253	0.311	0.533	1.078
	336	0.291	0.286	0.298	0.281	**0.278**	0.321	0.325	0.339	0.334	0.314	0.442	1.363	1.549
	720	0.393	0.378	0.393	0.397	**0.367**	0.408	0.421	0.433	0.417	0.414	0.675	3.379	2.631
ILI	24	**1.359**	2.063	1.617	2.215	1.522	2.317	3.228	3.483	2.294	2.527	8.313	5.764	4.400
	36	**1.405**	1.868	1.708	1.963	1.430	1.972	2.679	3.103	1.825	2.615	6.631	4.755	4.783
	48	**1.442**	1.790	1.633	2.130	1.673	2.238	2.622	2.669	2.010	2.359	7.299	4.763	4.832
	60	1.603	1.979	2.106	2.368	**1.529**	2.027	2.857	2.770	2.178	2.487	7.283	5.264	4.882

Table 10: **Full Few-shot Learning Results on 5% Data.** We use prediction length $O \in \{96, 192, 336, 720\}$. A lower MSE indicates better performance, and the best results are highlighted in **red**. '-' means that 5% time series is not sufficient to constitute a training set.

Methods		aLLM4TS		GPT4TS		DLinear		PatchTST		TimesNet		FEDformer		Autoformer		Stationary		ETSformer		LightTS		Informer		Reformer	
Metric		MSE	MAE	MSE	MAE	MSE	MAE	MSE	MAE	MSE	MAE	MSE	MAE	MSE	MAE	MSE	MAE	MSE	MAE	MSE	MAE	MSE	MAE	MSE	MAE
ETTh1	96	0.553	0.479	0.543	0.506	0.547	0.503	0.557	0.519	0.892	0.625	0.593	0.529	0.681	0.570	0.952	0.650	1.169	0.832	1.483	0.91	1.225	0.812	1.198	0.795
	192	0.597	0.498	0.748	0.580	0.720	0.604	0.711	0.570	0.940	0.665	0.652	0.563	0.725	0.602	0.943	0.645	1.221	0.853	1.525	0.93	1.249	0.828	1.273	0.853
	336	0.674	0.544	0.754	0.595	0.984	0.727	0.816	0.619	0.945	0.653	0.731	0.594	0.761	0.624	0.935	0.644	1.179	0.832	1.347	0.87	1.202	0.811	1.254	0.857
	720	-	-	-	-	-	-	-	-	-	-	-	-	-	-	-	-	-	-	-	-	-	-	-	-
	Avg.	**0.608**	**0.507**	0.681	0.560	0.750	0.611	0.694	0.569	0.925	0.647	0.658	0.562	0.722	0.598	0.943	0.646	1.189	0.839	1.451	0.903	1.225	0.817	1.241	0.835
ETTh2	96	0.331	0.392	0.376	0.421	0.442	0.456	0.401	0.421	0.409	0.420	0.390	0.424	0.428	0.468	0.408	0.423	0.678	0.619	2.022	1.006	3.837	1.508	3.753	1.518
	192	0.374	0.417	0.418	0.441	0.617	0.542	0.452	0.455	0.483	0.464	0.457	0.465	0.496	0.504	0.497	0.468	0.845	0.697	3.534	1.348	3.975	1.933	3.516	1.473
	336	0.418	0.443	0.408	0.439	1.424	0.849	0.464	0.469	0.499	0.479	0.477	0.483	0.486	0.496	0.507	0.481	0.905	0.727	4.063	1.451	3.956	1.520	3.312	1.427
	720	-	-	-	-	-	-	-	-	-	-	-	-	-	-	-	-	-	-	-	-	-	-	-	-
	Avg.	**0.374**	**0.417**	0.400	0.433	0.827	0.615	0.439	0.448	0.463	0.454	0.441	0.457	0.47	0.489	0.470	0.457	0.809	0.681	3.206	1.268	3.922	1.653	3.527	1.472
ETTm1	96	0.372	0.387	0.386	0.405	0.332	0.374	0.399	0.414	0.606	0.518	0.628	0.544	0.726	0.578	0.823	0.587	1.031	0.747	1.048	0.733	1.130	0.775	1.234	0.798
	192	0.407	0.405	0.440	0.438	0.358	0.390	0.441	0.436	0.681	0.539	0.666	0.566	0.750	0.591	0.844	0.591	1.087	0.766	1.097	0.756	1.150	0.788	1.287	0.839
	336	0.433	0.421	0.485	0.459	0.402	0.416	0.499	0.467	0.786	0.597	0.807	0.628	0.851	0.659	0.870	0.603	1.138	0.787	1.147	0.775	1.198	0.809	1.288	0.842
	720	0.464	0.442	0.577	0.499	0.511	0.489	0.767	0.587	0.796	0.593	0.822	0.633	0.857	0.655	0.893	0.611	1.245	0.831	1.200	0.799	1.175	0.794	1.247	0.828
	Avg.	0.419	**0.414**	0.472	0.450	**0.400**	0.417	0.526	0.476	0.717	0.561	0.730	0.592	0.796	0.620	0.857	0.598	1.125	0.782	1.123	0.765	1.163	0.791	1.264	0.826
ETTm2	96	0.214	0.293	0.199	0.280	0.236	0.326	0.206	0.288	0.220	0.299	0.229	0.320	0.232	0.322	0.238	0.316	0.404	0.485	1.108	0.772	3.599	1.478	3.883	1.545
	192	0.268	0.322	0.256	0.316	0.306	0.373	0.264	0.324	0.311	0.361	0.394	0.361	0.291	0.357	0.298	0.349	0.479	0.521	1.317	0.850	3.578	1.475	3.553	1.484
	336	0.305	0.355	0.318	0.353	0.380	0.423	0.334	0.367	0.338	0.366	0.378	0.427	0.478	0.517	0.353	0.380	0.552	0.555	1.415	0.879	3.561	1.473	3.446	1.460
	720	0.401	0.412	0.460	0.436	0.674	0.583	0.454	0.432	0.509	0.465	0.523	0.510	0.553	0.538	0.475	0.445	0.701	0.627	1.822	0.984	3.896	1.533	3.445	1.460
	Avg.	**0.297**	**0.345**	0.308	0.346	0.399	0.426	0.314	0.352	0.344	0.372	0.381	0.404	0.388	0.433	0.341	0.372	0.534	0.547	1.415	0.871	3.658	1.489	3.581	1.487

D.4. Detailed Results for Short-term Forecasting

Our comprehensive short-term forecasting results are showcased in Tab. 11. Throughout various scenarios, aLLM4TS consistently outperforms the majority of baseline models. Notably, we achieve a substantial improvement over GPT4TS, with notable margins such as **3.80%** overall, **8.54%** on M4-Yearly, and an average of **4.73%** on M4-Hourly, M4-Daily, and M4-Weekly. In comparison to the recent state-of-the-art forecasting models (N-HiTS and PatchTST), aLLM4TS also demonstrates comparable or superior performance.

D.5. Comparison with Traditional Methods on Few-shot Learning

Deep learning approaches provide benefits over traditional methods for managing extensive datasets; nonetheless, in the context of few-shot learning, it is imperative to also acknowledge the relevance of traditional methods. As depicted in Table 12, aLLM4TS still demonstrates superior performance.

D.6. Full Ablation Results and Analysis

In this section, we conduct several ablations on framework design and the effectiveness of our two-stage forecasting-based pre-training. Full results are in Tab. 13.

Casual Next-Patch Continual Pre-training. Comparing row A.1 and B.1 in Tab. 13, an average MSE increase of **8.80**% is observed, indicating that ablating casual next-patch continual pre-training significantly harms the sequence pattern recognition and representation modeling of the LLM for effective time series forecasting. We attribute it to the inadequate adaption to apply pre-trained LLMs in time series without alignment that fits the time series dynamics and the inherited casual modeling within LLMs.

LLM Pre-trained Weight. We designed two sets of ablation experiments with different model sizes to avoid the mismatch between training data and model parameter quantity. We discard the pre-trained weights of the LLMs and train from scratch the first 6 layers (**B.2**) and the first 3 layers (**B.3**) of GPT-2. Ablating the LLM pre-trained weights directly results in the loss of the learned sequential representation capabilities from massive sequential text data (Zhou et al., 2023; Gruver et al., 2024). Consequently, it becomes difficult to learn the temporal representation from scratch within the LLM architecture, leading to the degradation in performance of **5.15**% and **7.91**%, respectively.

Patch-level Decoder. In ablation experiment **C.1**, we employed the conventional sequence-level decoder, resulting in an

Table 11: **Full Results of Short-term Forecasting.** A lower value indicates better performance. **Red**: the best.

	Methods	aLLM4TS	GPT4TS	TimesNet	PatchTST	N-HiTS	N-BEATS	ETSformer	LightTS	DLinear	FEDformer	Stationary	Autoformer	Informer	Reformer
Yearly	SMAPE	13.540	14.804	**13.387**	13.477	13.418	13.436	18.009	14.247	16.965	13.728	13.717	13.974	14.727	16.169
	MASE	3.108	3.608	**2.996**	3.019	3.045	3.043	4.487	3.109	4.283	3.048	3.078	3.134	3.418	3.800
	OWA	0.805	0.907	**0.786**	0.792	0.793	0.794	1.115	0.827	1.058	0.803	0.807	0.822	0.881	0.973
Quarterly	SMAPE	10.216	10.508	**10.100**	10.38	10.202	10.124	13.376	11.364	12.145	10.792	10.958	11.338	11.360	13.313
	MASE	1.1971	1.233	**1.182**	1.233	1.194	1.169	1.906	1.328	1.520	1.283	1.325	1.365	1.401	1.775
	OWA	0.900	0.927	**0.890**	0.921	0.899	0.886	1.302	1.000	1.106	0.958	0.981	1.012	1.027	1.252
Monthly	SMAPE	12.775	12.981	**12.670**	12.959	12.791	12.677	14.588	14.014	13.514	14.260	13.917	13.958	14.062	20.128
	MASE	0.944	0.956	**0.933**	0.970	0.969	0.937	1.368	1.053	1.037	1.102	1.097	1.103	1.141	2.614
	OWA	0.887	0.899	**0.878**	0.905	0.899	0.880	1.149	0.981	0.956	1.012	0.998	1.002	1.024	1.927
Others	SMAPE	5.032	5.282	**4.891**	4.952	5.061	4.925	7.267	15.880	6.709	4.954	6.302	5.485	24.460	32.491
	MASE	3.481	3.573	3.302	3.347	**3.216**	3.391	5.240	11.434	4.953	3.264	4.064	3.865	20.960	33.355
	OWA	1.078	1.119	**1.035**	1.049	1.040	1.053	1.591	3.474	1.487	1.036	1.304	1.187	5.879	8.679
Average	SMAPE	11.950	12.422	**11.829**	12.059	11.927	11.851	14.718	13.525	13.639	12.840	12.780	12.909	14.086	18.200
	MASE	1.629	1.763	**1.585**	1.623	1.613	1.599	2.408	2.111	2.095	1.701	1.756	1.771	2.718	4.223
	OWA	0.867	0.919	**0.851**	0.869	0.861	0.855	1.172	1.051	1.051	0.918	0.930	0.939	1.230	1.775

Table 12: **Comparison with Traditional Methods.** A lower value indicates better performance. **Red**: the best, Underlined: the second best.

Methods		aLLM4TS 5%		ETS		ARIMA		NaiveDrift	
Metric		MSE	MAE	MSE	MAE	MSE	MAE	MSE	MAE
ETTh2	96	**0.331**	**0.392**	2.954	0.742	0.481	0.443	0.764	0.561
	192	**0.374**	**0.417**	10.226	1.212	0.585	0.495	1.560	0.785
ETTm1	96	**0.413**	**0.397**	52.237	2.689	0.693	0.547	1.539	0.913
	192	**0.416**	**0.399**	186.445	4.654	0.710	0.557	2.869	1.215

Table 13: **Full Ablation Results on 4 ETT Datasets in Long-term Forecasting.** **Red**: the best, Underlined: the second best.

Methods		**A.1** aLLM4TS		**A.2** aLLM4TS (3)		**A.3** aLLM4TS (9)		**A.4** aLLM4TS (12)		**B.1** w/o Casual Continual Pretraining		**B.2** w/o LLM Pretrained Weights (6)		**B.3** w/o LLM Pretrained Weights (3)		**C.1** w/o Patch-level Decoder		**C.2** w/o Position -aware Attention Mask		**D.1** Init with FFT		**D.2** Init with Random		**E.1** LN+PE+Attn		**E.2** LN+PE+ Attn+FFN	
Metric		MSE	MAE	MSE	MAE	MSE	MAE	MSE	MAE	MSE	MAE	MSE	MAE	MSE	MAE	MSE	MAE	MSE	MAE	MSE	MAE	MSE	MAE	MSE	MAE	MSE	MAE
ETTh1	96	0.380	0.407	0.410	0.437	0.412	0.436	0.575	0.527	0.444	0.459	0.410	0.435	0.432	0.455	0.412	0.425	0.419	0.435	0.380	0.406	0.378	0.406	0.408	0.442	0.424	0.440
	192	0.396	0.417	0.419	0.444	0.434	0.448	0.573	0.530	0.450	0.466	0.419	0.442	0.444	0.464	0.447	0.445	0.435	0.437	0.407	0.422	0.415	0.425	0.424	0.451	0.444	0.451
	336	0.413	0.428	0.429	0.453	0.452	0.461	0.570	0.535	0.450	0.473	0.431	0.453	0.455	0.475	0.457	0.463	0.438	0.455	0.421	0.434	0.458	0.448	0.439	0.461	0.463	0.463
	720	0.461	0.462	0.488	0.490	0.508	0.495	0.602	0.558	0.496	0.506	0.487	0.489	0.515	0.514	0.502	0.496	0.481	0.487	0.454	0.461	0.537	0.504	0.496	0.495	0.527	0.500
	Avg.	**0.413**	**0.429**	0.437	0.456	0.452	0.460	0.580	0.533	0.460	0.476	0.437	0.455	0.462	0.477	0.455	0.457	0.443	0.454	0.416	0.431	0.447	0.446	0.442	0.462	0.465	0.464
ETTh2	96	0.251	0.332	0.259	0.335	0.274	0.344	0.273	0.344	0.292	0.360	0.263	0.342	0.266	0.345	0.330	0.386	0.297	0.365	0.274	0.347	0.281	0.353	0.275	0.345	0.272	0.341
	192	0.298	0.363	0.305	0.367	0.319	0.374	0.313	0.371	0.329	0.386	0.303	0.363	0.310	0.376	0.400	0.426	0.330	0.388	0.323	0.379	0.325	0.380	0.320	0.374	0.319	0.371
	336	0.343	0.396	0.344	0.398	0.348	0.399	0.339	0.393	0.352	0.407	0.352	0.402	0.355	0.413	0.380	0.425	0.351	0.407	0.369	0.413	0.362	0.408	0.358	0.404	0.363	0.404
	720	0.417	0.450	0.411	0.444	0.414	0.446	0.411	0.442	0.427	0.456	0.427	0.458	0.423	0.459	0.438	0.461	0.452	0.466	0.454	0.470	0.437	0.459	0.429	0.453	0.438	0.458
	Avg.	**0.327**	**0.385**	0.330	0.386	0.339	0.391	0.334	0.388	0.350	0.402	0.336	0.391	0.339	0.398	0.387	0.425	0.358	0.407	0.355	0.402	0.351	0.400	0.346	0.394	0.348	0.394
ETTm1	96	0.290	0.361	0.287	0.361	0.341	0.391	0.341	0.393	0.314	0.367	0.307	0.365	0.311	0.370	0.301	0.357	0.342	0.393	0.321	0.373	0.308	0.364	0.300	0.360	0.301	0.358
	192	0.316	0.376	0.327	0.375	0.381	0.412	0.379	0.413	0.350	0.389	0.342	0.385	0.348	0.391	0.344	0.384	0.381	0.416	0.352	0.392	0.341	0.384	0.337	0.383	0.334	0.379
	336	0.342	0.391	0.366	0.397	0.420	0.432	0.417	0.433	0.387	0.409	0.377	0.404	0.387	0.412	0.375	0.403	0.413	0.433	0.387	0.411	0.375	0.403	0.376	0.403	0.370	0.399
	720	0.381	0.414	0.421	0.427	0.475	0.459	0.474	0.460	0.441	0.438	0.431	0.433	0.444	0.441	0.427	0.431	0.459	0.456	0.441	0.440	0.434	0.433	0.438	0.434	0.427	0.428
	Avg.	**0.332**	**0.386**	0.350	0.390	0.404	0.424	0.403	0.425	0.373	0.401	0.364	0.397	0.373	0.404	0.362	0.394	0.399	0.425	0.375	0.404	0.365	0.396	0.363	0.395	0.358	0.391
ETTm2	96	0.212	0.307	0.205	0.300	0.219	0.308	0.218	0.309	0.230	0.323	0.214	0.308	0.219	0.306	0.185	0.271	0.223	0.311	0.212	0.307	0.233	0.323	0.232	0.316	0.208	0.302
	192	0.263	0.337	0.255	0.330	0.274	0.342	0.271	0.339	0.276	0.350	0.267	0.336	0.278	0.347	0.257	0.316	0.273	0.341	0.269	0.338	0.279	0.349	0.288	0.347	0.268	0.342
	336	0.310	0.365	0.316	0.369	0.327	0.375	0.322	0.370	0.321	0.376	0.319	0.366	0.326	0.376	0.311	0.359	0.320	0.370	0.319	0.369	0.322	0.374	0.338	0.377	0.324	0.377
	720	0.393	0.414	0.391	0.410	0.409	0.426	0.402	0.418	0.400	0.421	0.403	0.415	0.397	0.414	0.383	0.403	0.398	0.416	0.403	0.416	0.401	0.419	0.417	0.423	0.406	0.426
	Avg.	0.294	0.356	0.292	0.352	0.307	0.363	0.303	0.359	0.307	0.368	0.301	0.356	0.305	0.361	**0.284**	**0.337**	0.303	0.335	0.301	0.358	0.309	0.366	0.319	0.366	0.302	0.362

average performance loss exceeding **8.54**%. Despite using a decoder over 100 times larger and can train specifically for each input/output length, a substantial performance loss occurred. This is attributed to the potential downstream task overfitting of the huge sequence-level head and the incapability to disentangle the patch representation encoding and decoding process, leading to inadequate patch representation optimization in the LLM backbone.

Position-aware Attention Mask. In aLLM4TS, we transform the forecasting into multi-patch representation optimization based on well-aligned patch-based time series knowledge. Position-aware attention mask is designed to further enhance the optimization process by removing the unwanted confusion brought by other being-optimized anchors during the optimization. Ablation of this component (**C.2**) results in over **10.01**% performance deterioration.

The Number of LLM Layers. To better balance performance and computational efficiency, we test using various numbers of layers on ETT datasets (**A.2**, **A.3**, **A.4**). Shallow layers typically operate on modeling coarse-grained token sequence features, which is advantageous for optimizing time series representations (Ethayarajh, 2019). In contrast, deep layers often focus more on domain-specific sequence relationships, which can pose challenges for transferring sequence modeling capabilities to time series. Thus GPT-2 with 6 layers is chosen as our default backbone.

Non-parametric Methods to Initialize the Anchors. During stage 2, we employ non-parametric methods to initialize the anchors to be predicted. This initialization includes recent historical values by default and the discrete Fourier decomposition values for the look-back window (**D.1**) and random values (**D.2**). It is observed that as the noisy information in the initial anchor values increases, the representation optimization becomes more challenging, leading to respective increases in MSE loss of **6.16**% and **7.65**%.

Unfrozen Parts in LLM. By default, we only unfreeze the layer normalization layer and position embedding to boost downstream forecasting optimization in stage 2, which is considered a common practice (Lu et al., 2022; Houlsby et al., 2019) to adapt llm in other sequence modeling tasks. In ablation **E.1** and **E.2**, we try to fine-tune other parts like the attention layers or FFN layers but end with the poor performance of more than **7.67**% MSE increase. We attribute this to overfitting caused by ineffective training due to limited data in downstream tasks.

D.7. Full Results of Interpretability Experiment

We conducted case studies on the Traffic, Electricity, and Weather datasets to illustrate the evolution of attention weights from the prediction horizon patches to look-back window patches at four stages in Fig. 6, Fig. 7 and Fig. 8. The 4 subplots in each figure detail the attention weights optimization process from randomly-initialized (Stage ❶), through LLMs-pre-trained (Stage ❷), casually next-patch continual pre-trained (Stage ❸) to multi-patch prediction adaption (Stage ❹). Our whole observations are as follows: **Obs.① After stage ❹, aLLM4TS adeptly captures the complex multi-periodic properties of time series and a discernible trend of increasing information importance along the temporal dimension.** This is evidently observed in all Fig. 6 (d), Fig. 7 (d) and Fig. 8 (d). Among these, look-back window patches closest to the prediction horizon exhibit similar attention patterns from prediction horizon patches at time steps t, $t+3$, and $\cdots$. With a patch size of 16 and a stride of 8, sampling hourly, this corresponds to local day cycles. Additionally, there exist 20 patch cycles (equivalent to 168 hours), indicating weekly cycles. Furthermore, look-back window patches closer to the predicted horizon receive increasing attention due to their temporal proximity, indicating their greater informational significance. **Obs.② After stage ❸, aLLM4TS effectively learns universal single-period features (e.g., day) and showcases a noticeable trend of increasing attention along the time dimension**, especially in Traffic in Fig. 6 (c) and Electricity in Fig. 7 (c) which possess more pronounced periodicity, stemming from the process of casually predicting the next patch. **Obs.③ Pre-trained LLM parameters capture fundamental individual cycle attributes within time series,** offering notable optimization benefits when contrasted with random initialization, thereby serving as a robust optimization reference for downstream time-series representation optimization.

D.8. Further Exploration Experiment on Pre-trained LLMs

To further demonstrate the significance of pre-training LLM weights for time series representation learning, we highlight that the sequence modeling abilities obtained from extensive text data serve as effective initial anchors for time series representation optimization. In addition to assessing the impact of LLM pre-training parameters in ablation experiments B.2 and B.3 in Sec. 5.7, and examining the pre-training LLMs' ability to capture fundamental periodicities in time series through the interpretability experiment in Sec. 5.8, we adopted SOTA transformer-based patchTST (Nie et al., 2023) as the model backbone and conducted same two-stage experiments as aLLM4TS in Sec. 4. The results underscore the utility of pre-training LLM weights as a robust optimization foundation for time series analysis tasks, facilitating the adaptation of sequence modeling skills acquired from vast text data to time series representation learning.

Specifically, we initialized a patchTST and conducted identical two-stage training as aLLM4TS in Sec. 4, encompassing casual next-patch pre-training in the first stage and multi-patch prediction adaption in the second stage. Experimental

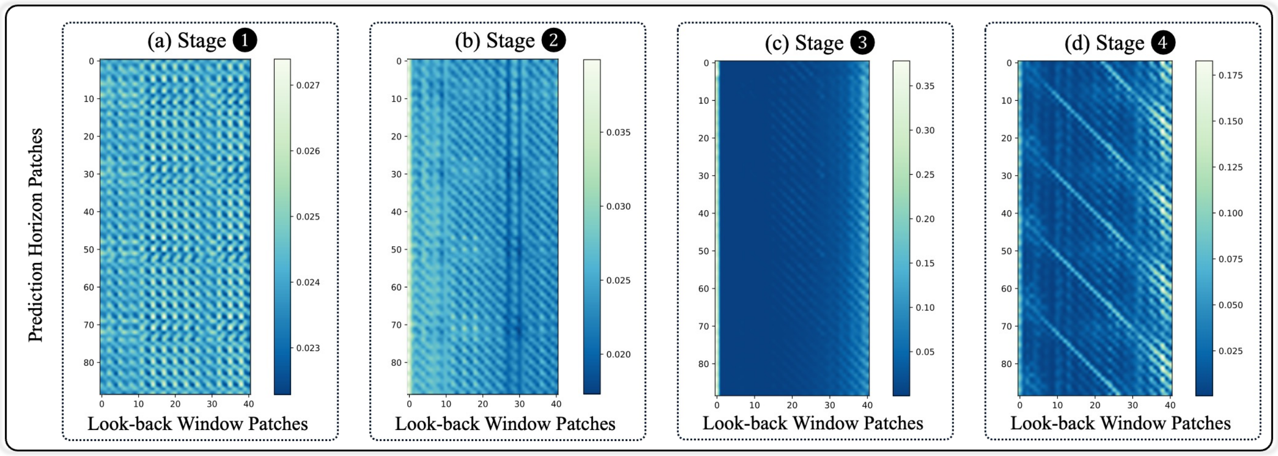

Figure 6: Case study of Traffic Dataset. The Y-axis and X-axis represent prediction horizon patch indexes and look-back window patch indexes, respectively.

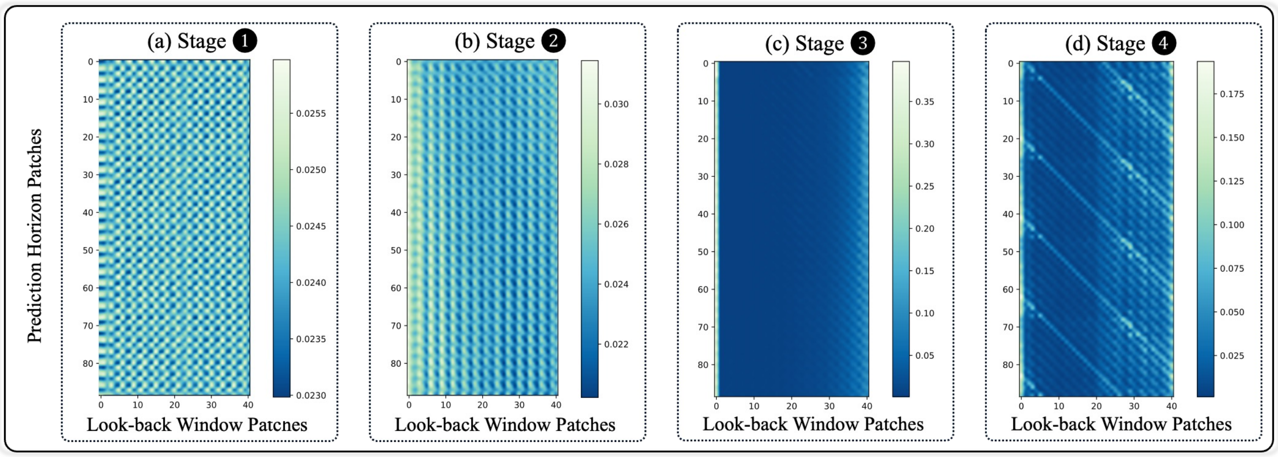

Figure 7: Case study of Electricity Dataset. The Y-axis and X-axis represent prediction horizon patch indexes and look-back window patch indexes, respectively.

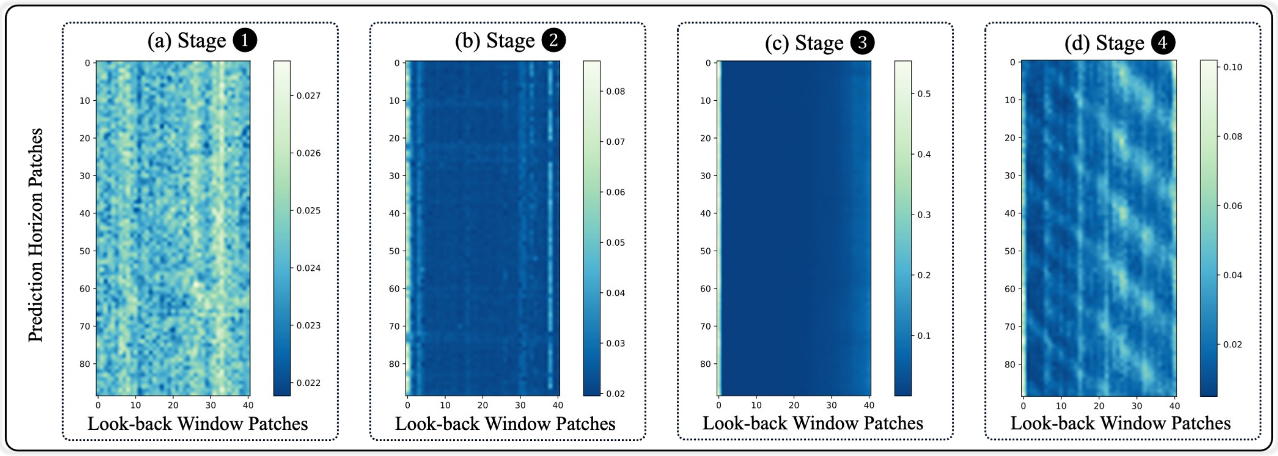

Figure 8: Case study of Weather Dataset. The Y-axis and X-axis represent prediction horizon patch indexes and look-back window patch indexes, respectively.

configurations remained consistent, with the first stage pre-training executed on the Weather, Traffic, Electricity, ILI, and 4 ETT datasets, followed by a representation adaptation and prediction on the 4 ETT datasets. Results in Tab. 14 reveal that patchTST without pre-training weights from extensive text data, while showing improvement throughout the two-stage training, still exhibits a discernible disparity compared to aLLM4TS with pre-training weights from extensive text data. This divergence can be attributed to the inadequacy of limited time series data to facilitate learning universal time series representations from the challenging pre-training tasks, whereas the sequence modeling proficiency acquired from text-based LLM pre-training weights offers a solid initialization basis, enabling effective optimization of time series representations despite limited time series data availability. This experiment, along with the ablation experiments (B.2 and B.3) in Sec. 5.7 and the interpretability experiment in Sec. 5.8, collectively emphasize the crucial significance of LLM pre-training weights in learning time series representations, both quantitatively and qualitatively.

Table 14: Experiment results for special ablation on the role of PLM parameters. We use the MSE and MAE as the default metric. A lower value indicates better performance. aLLM4TS-GPT2 denotes the our default aLLM4TS with the pre-trained GPT-2 as model backbone. aLLM4TS-PatchTST denotes the ablated aLLM4TS with the PatchTST as model backbone.

Methods		aLLM4TS-GPT2		aLLM4TS-PatchTST	
Datasets	Horizon	MSE	MAE	MSE	MAE
$ETTh1$	96	0.380	0.376	0.408	0.435
	192	0.396	0.416	0.427	0.455
	336	0.413	0.442	0.440	0.476
	720	0.461	0.477	0.500	0.517
$ETTh2$	96	0.251	0.285	0.317	0.380
	192	0.298	0.354	0.339	0.396
	336	0.343	0.373	0.350	0.408
	720	0.417	0.406	0.440	0.463
$ETTm1$	96	0.290	0.292	0.347	0.378
	192	0.316	0.332	0.382	0.396
	336	0.342	0.366	0.425	0.419
	720	0.381	0.417	0.490	0.455
$ETTm2$	96	0.171	0.173	0.244	0.327
	192	0.234	0.229	0.285	0.350
	336	0.291	0.286	0.327	0.374
	720	0.393	0.378	0.406	0.417

D.9. Further Exploration Experiment on Patch-wise Decoding

After PatchTST (Nie et al., 2023) proposed to utilize patches as the foundational unit for time series processing, owing to their capacity to capture local semantic information while minimizing memory usage, the adoption of patches as the core processing unit for time series analysis tasks has become widespread (Cao et al., 2024; Dong et al., 2023; Lee et al., 2023). However, previous patch-based models have predominantly focused on devising diverse encoder model architectures, overlooking the design of the final decoding layer. These models typically employ a simple approach: after generating a sequence of patches representation $\{\boldsymbol{p}_1, \cdots, \boldsymbol{p}_{L_p}\}, \boldsymbol{p}_i \in \mathbb{R}^D$ across L_p patches with dimension D from the model backbone, these patches are concatenated and unfolded into a one-dimensional sequence, followed by a large sequence-wise layer $\mathbf{W}_s \in \mathbb{R}^{(L_p \cdot D) \times H}$ to decode the patch representation into prediction horizon H. Yet, two issues necessitate attention: (1) **the extensive linear decoding layer might lead to insufficient training of the model backbone and overfitting risks to downstream tasks**; (2) **the fully connected linear layer fails to disentangle the patch encoding and decoding processes**, hindering the optimization of patch representations by the model backbone and exacerbating overfitting of this fully connected layer to downstream tasks.

In our aLLM4TS, we introduce a patch-wise decoder $\mathbf{W}_p \in \mathbb{R}^{D \times P}$ to naturally tackle these challenges, reducing the parameter size to only $\frac{P}{L*H}$ (*e.g.*, 0.34%, when $P = 16, L_p = 64, H = 720$) of previous sequence-wise decoding layers while disentangling the patch representation encoding and decoding processes. P denotes the patch size. This empowers the LLM backbone and patch-wise decoder to excel in their respective roles: enhancing the representation of each patch and autonomously decoding each patch into the temporal domain. Additionally, we conduct supplementary experiments to elucidate the deficiencies of previous models with sequence-level decoding, confirming that their model performance primarily overfits to the final large fully connected linear layer. Specifically, by initializing the state-of-the-art time series analysis model based on patches, PatchTST, with all other configurations unchanged except for substituting the final sequence-level decoding linear layer with a patch-wise decoding linear layer, the experimental results in Tab. 15 reveal a performance deterioration of over 37.6%. This underscores the considerable risk of overfitting associated with the sequence-wise linear layer commonly employed in the past, as well as the inadequate optimization of the model backbone.

Table 15: Experiment results for ablation of patch-wise decoding in PatchTST. We use the MSE and MAE as the default metric. A lower value indicates better performance. PatchTST-sd denotes the origin PatchTST with the sequence-wise decoding layer. PatchTST-pd denotes the PatchTST with our patch-wise decoding layer.

Methods		PatchTST-sd		PatchTST-pd	
Datasets	Horizon	MSE	MAE	MSE	MAE
$ETTh1$	96	0.375	0.399	0.498	0.489
	192	0.414	0.421	0.497	0.492
	336	0.431	0.436	0.496	0.498
	720	0.449	0.466	0.533	0.527
$ETTh2$	96	0.274	0.336	0.287	0.362
	192	0.339	0.379	0.305	0.381
	336	0.331	0.380	0.335	0.396
	720	0.379	0.422	0.414	0.446
$ETTm1$	96	0.290	0.342	0.586	0.517
	192	0.332	0.369	0.595	0.522
	336	0.255	0.392	0.606	0.528
	720	0.420	0.424	0.626	0.539
$ETTm2$	96	0.165	0.255	0.275	0.344
	192	0.220	0.292	0.305	0.361
	336	0.278	0.329	0.341	0.380
	720	0.367	0.385	0.420	0.423

D.10. Further Exploration Experiment on Look-back Window Length

In the first stage of aLLM4TS, referred to as casual next-patch pre-training, we provide a specified number of patch sequences where each patch casually predicts the next patch. The default look-back window length for this patch sequence is set to 720. However, considering the long-term forecasting tasks downstream, where the default value of the look-back window length is 336 and the prediction horizon length is 720, the sum of these two exceeds the maximum length of the continual casual next-patch pre-training. This inconsistency might cause a drop in performance in downstream tasks due to the extra workload of the look-back window length shift, including inadequate adjustment of position embedding, among other factors. We extended the look-back window length in the first-stage causal next-patch pre-training from 720 to 1024, maintaining consistency with Sec. 5.2 for other settings. Comparative experiments were performed in downstream tasks involving long-term forecasting and imputation, with results presented in Tab. 16 and Tab. 17. It is evident that augmenting the look-back window length in the first stage can effectively alleviate inconsistencies in the observable horizon between upstream and downstream tasks of aLLM4TS, thereby improving the model's overall performance, particularly for long-term prediction horizons, such as a prediction horizon of 720.

Table 16: Experiment results for the influence of longer look-back window in long-term forecasting. We use the MSE as the default metric. A lower value indicates better performance. We use forecasting horizons $H \in \{96, 192, 336, 720\}$. aLLM4TS-origin(longer) denotes the aLLM4TS with look-back window length as 720(1024) in casual next-patch pre-training.

Datasets	Weather-96	Weather-192	Weather-336	Weather-720	ETTh2-96	ETTh2-192	ETTh2-336	ETTh2-720	ETTm2-96	ETTm2-192	ETTm2-336	ETTm2-720
aLLM4TS-origin	0.149	0.190	0.238	0.316	0.251	0.298	0.343	0.417	0.171	0.234	0.291	0.403
aLLM4TS-longer	0.148	0.187	0.236	0.317	0.252	0.301	0.345	0.408	0.175	0.240	0.293	0.394

D.11. Detailed Results for Classification

To assess the performance of the representations learned by aLLM4TS in high-level abstract representation tasks and their generalizability across datasets, we evaluated aLLM4TS at the sequence level after stage 1 casual next-patch pre-training,

Table 17: Experiment results for the influence of longer look-back window in imputation. We use the MSE and MAE as the default metric. A lower value indicates better performance. aLLM4TS-origin(longer) denotes the aLLM4TS with look-back window length as 720(1024) in casual next-patch pre-training.

Methods		aLLM4TS-origin		aLLM4TS-longer	
Mask	Ratio	MSE	MAE	MSE	MAE
ETTh1	12.5%	0.041	0.139	0.040	0.137
	25%	0.056	0.161	0.055	0.157
	37.5%	0.073	0.182	0.072	0.181
	50%	0.098	0.210	0.097	0.209
ETTh2	12.5%	0.040	0.126	0.040	0.125
	25%	0.046	0.138	0.046	0.138
	37.5%	0.051	0.147	0.052	0.147
	50%	0.060	0.159	0.060	0.158
ETTm1	12.5%	0.019	0.093	0.019	0.091
	25%	0.025	0.104	0.024	0.102
	37.5%	0.032	0.118	0.031	0.115
	50%	0.045	0.139	0.044	0.137
ETTm2	12.5%	0.019	0.079	0.019	0.078
	25%	0.022	0.086	0.021	0.085
	37.5%	0.024	0.092	0.024	0.092
	50%	0.028	0.100	0.027	0.100

using pre-training data consistent with long-term forecasting in Sec. 5.2. Specifically, we adopted the experiment settings outlined in GPT4TS: For classification, we utilized 10 multivariate UEA classification datasets (Bagnall et al., 2018) encompassing gesture, action, audio recognition, medical diagnosis, and other practical tasks. Full classification experiment results are in Tab. 18.

Table 18: Full results for the classification task. We use the accuracy as default metric. A higher value indicates better performance. **Red**: the best, Underlined: the second best. We compare our aLLM4TS with SOTA LLM-based GPT4TS, CNN-based TimesNet, MLP-based DLinear and Machine-Learning-based XGBoost.

Methods	aLLM4TS	GPT4TS	TimesNet	DLinear	XGBoost
EthanolConcentration	33.5	31.2	32.7	32.6	**43.7**
FaceDetection	68.3	68.2	**68.6**	68.0	63.3
Handwriting	27.5	20.6	**32.8**	27.0	15.8
Heartbeat	**78.0**	76.6	75.6	75.1	73.2
JapaneseVowels	96.8	**97.6**	97.3	96.2	86.5
PEMS-SF	64.7	60.7	89.6	75.1	**98.3**
SelfRegulationSCP1	**92.5**	90.8	87.7	87.3	84.6
SelfRegulationSCP2	**57.2**	54.3	56.1	50.5	48.9
SpokenArabicDigits	**99.0**	**99.0**	98.8	81.4	69.6
UWaveGestureLibrary	85.3	85.9	**86.9**	82.1	75.9

D.12. Detailed Results for Imputation

We perform experiments on four ETT datasets (ETTh1, ETTh2, ETTm1, ETTm2), each exhibiting common data-missing scenarios. Adhering to the GPT4TS configurations, we assess different random mask ratios ($\{12.5\%, 25\%, 37.5\%, 50\%\}$) for evaluating diverse levels of missing data.

The results, presented in Tab. 19, affirm that aLLM4TS excels in performance across the majority of datasets. Notably, when contrasted with the prior state-of-the-art models TimesNet and GPT4TS, aLLM4TS demonstrates more than **9.19%** decrease in mean squared error (MSE) for ETTh1 and competitive SOTA performance across the four benchmark datasets. This substantiates the efficacy of the proposed approach in discerning temporal patterns within incomplete time series.

Table 19: **Brief Results for Imputation Task.** We randomly mask {12.5%, 25%, 37.5%, 50%} time points of 96-length time series. The results are averaged from 4 different mask ratios. A lower value indicates better performance. **Red**: the best, Underlined: the second best.

Methods	aLLM4TS		GPT4TS		TimesNet		PatchTST		ETSformer		LightTS		DLinear		FEDformer		Stationary		Autoformer		Informer		Reformer	
	MSE	MAE	MSE	MAE	MSE	MAE	MSE	MAE	MSE	MAE	MSE	MAE	MSE	MAE	MSE	MAE	MSE	MAE	MSE	MAE	MSE	MAE	MSE	MAE
ETTh1	**0.067**	**0.172**	0.070	0.175	0.078	0.187	0.115	0.224	0.202	0.329	0.284	0.373	0.201	0.306	0.117	0.246	0.094	0.201	0.103	0.214	0.161	0.279	0.122	0.245
ETTh2	**0.049**	**0.142**	0.050	0.145	0.049	0.146	0.065	0.163	0.367	0.436	0.119	0.250	0.142	0.259	0.163	0.279	0.053	0.152	0.055	0.156	0.337	0.452	0.234	0.352
ETTm1	0.031	0.113	0.029	0.107	**0.027**	**0.107**	0.047	0.140	0.120	0.253	0.104	0.218	0.093	0.206	0.062	0.177	0.036	0.126	0.051	0.150	0.071	0.188	0.055	0.166
ETTm2	0.023	0.089	0.023	0.087	**0.022**	**0.088**	0.029	0.102	0.208	0.327	0.046	0.151	0.096	0.208	0.101	0.215	0.026	0.099	0.029	0.105	0.156	0.292	0.157	0.280

Table 20: **Full Results for the Imputation Task.** A lower value indicates better performance. **Red**: the best, Underlined: the second best.

Methods		aLLM4TS		GPT4TS		TimesNet		PatchTST		ETSformer		LightTS		DLinear		FEDformer		Stationary		Autoformer		Informer		Reformer	
Mask	Ratio	MSE	MAE	MSE	MAE	MSE	MAE	MSE	MAE	MSE	MAE	MSE	MAE	MSE	MAE	MSE	MAE	MSE	MAE	MSE	MAE	MSE	MAE	MSE	MAE
ETTh1	12.5%	0.041	0.139	0.043	0.142	0.057	0.159	0.093	0.201	0.126	0.263	0.240	0.345	0.151	0.267	0.070	0.190	0.060	0.165	0.074	0.182	0.114	0.234	0.074	0.194
	25%	0.056	0.161	0.057	0.160	0.069	0.178	0.107	0.217	0.169	0.304	0.265	0.364	0.180	0.292	0.106	0.236	0.080	0.189	0.090	0.203	0.140	0.262	0.102	0.227
	37.5%	0.073	0.182	0.074	0.183	0.084	0.196	0.120	0.230	0.220	0.347	0.296	0.382	0.215	0.318	0.124	0.258	0.102	0.212	0.109	0.222	0.174	0.293	0.135	0.261
	50%	0.098	0.210	0.107	0.216	0.102	0.215	0.141	0.248	0.293	0.402	0.334	0.404	0.257	0.347	0.165	0.299	0.133	0.240	0.137	0.248	0.215	0.325	0.179	0.298
	Avg	**0.067**	**0.172**	0.070	0.175	0.078	0.187	0.115	0.224	0.202	0.329	0.284	0.373	0.201	0.306	0.117	0.246	0.094	0.201	0.103	0.214	0.161	0.279	0.122	0.245
ETTh2	12.5%	0.040	0.126	0.041	0.129	0.040	0.130	0.057	0.152	0.187	0.319	0.101	0.231	0.100	0.216	0.095	0.212	0.042	0.133	0.044	0.138	0.305	0.431	0.163	0.289
	25%	0.046	0.138	0.046	0.139	0.046	0.141	0.061	0.158	0.279	0.390	0.115	0.246	0.127	0.247	0.137	0.258	0.049	0.147	0.050	0.149	0.322	0.444	0.206	0.331
	37.5%	0.051	0.147	0.053	0.150	0.052	0.151	0.067	0.166	0.400	0.465	0.126	0.257	0.158	0.276	0.187	0.304	0.056	0.158	0.060	0.163	0.353	0.462	0.252	0.370
	50%	0.060	0.159	0.060	0.160	0.060	0.162	0.073	0.174	0.602	0.572	0.136	0.268	0.183	0.299	0.232	0.341	0.065	0.170	0.068	0.173	0.369	0.472	0.316	0.419
	Avg	**0.049**	**0.142**	0.050	0.145	0.049	0.146	0.065	0.163	0.367	0.436	0.119	0.250	0.142	0.259	0.163	0.279	0.053	0.152	0.055	0.156	0.337	0.452	0.234	0.352
ETTm1	12.5%	0.019	0.093	0.018	0.089	0.023	0.101	0.041	0.130	0.096	0.229	0.093	0.206	0.080	0.193	0.052	0.166	0.032	0.119	0.046	0.144	0.063	0.180	0.042	0.146
	25%	0.025	0.104	0.023	0.099	0.023	0.101	0.044	0.135	0.096	0.229	0.093	0.206	0.080	0.193	0.052	0.166	0.032	0.119	0.046	0.144	0.063	0.180	0.042	0.146
	37.5%	0.032	0.118	0.030	0.111	0.029	0.111	0.049	0.143	0.133	0.271	0.113	0.231	0.103	0.219	0.069	0.191	0.039	0.131	0.057	0.161	0.079	0.200	0.063	0.182
	50%	0.045	0.139	0.041	0.130	0.036	0.124	0.055	0.151	0.186	0.323	0.134	0.255	0.132	0.248	0.089	0.218	0.047	0.145	0.067	0.174	0.093	0.218	0.082	0.208
	Avg	0.031	0.113	0.029	0.107	**0.027**	**0.107**	0.047	0.140	0.120	0.253	0.104	0.218	0.093	0.206	0.062	0.177	0.036	0.126	0.051	0.150	0.071	0.188	0.055	0.166
ETTm2	12.5%	0.019	0.079	0.018	0.078	0.018	0.080	0.026	0.094	0.108	0.239	0.034	0.127	0.062	0.166	0.056	0.159	0.021	0.088	0.023	0.092	0.133	0.270	0.108	0.228
	25%	0.022	0.086	0.021	0.084	0.020	0.085	0.028	0.099	0.164	0.294	0.042	0.143	0.085	0.196	0.080	0.195	0.024	0.096	0.026	0.101	0.135	0.272	0.136	0.262
	37.5%	0.024	0.092	0.024	0.091	0.023	0.091	0.030	0.104	0.237	0.356	0.051	0.159	0.106	0.222	0.110	0.231	0.027	0.103	0.030	0.108	0.155	0.293	0.175	0.300
	50%	0.028	0.100	0.027	0.098	0.026	0.098	0.034	0.110	0.323	0.421	0.059	0.174	0.131	0.247	0.156	0.276	0.030	0.108	0.035	0.119	0.200	0.333	0.211	0.329
	Avg	0.023	0.089	0.023	0.087	**0.022**	**0.088**	0.029	0.102	0.208	0.327	0.046	0.151	0.096	0.208	0.101	0.215	0.026	0.099	0.029	0.105	0.156	0.292	0.157	0.280

D.13. Detailed Results for Anomaly Detection

Table 21: **Full Results for the Anomaly Detection.** P represents Precision, R represents Recall, and F1 represents the F1-score. A higher value indicates better performance. **Red**: the best.

Methods	SMD			MSL			SMAP			SWaT			PSM			Avg F1
Metrics	P	R	F1	P	R	F1	P	R	F1	P	R	F1	P	R	F1	%
aLLM4TS	0.8787	0.8309	85.42	81.58	82.95	82.26	85.40	**71.84**	**78.04**	**97.90**	92.53	**94.57**	98.47	**95.94**	97.19	**87.51**
GPT4TS	88.89	**84.98**	**86.89**	82.00	82.91	82.45	90.60	60.95	72.88	92.20	96.34	94.23	98.62	95.68	97.13	86.72
TimesNet	87.91	81.54	84.61	**89.54**	75.36	81.84	90.14	56.40	69.39	90.75	95.40	93.02	98.51	95.20	**97.34**	85.24
PatchTST	87.26	82.14	84.62	88.34	70.96	78.70	90.64	55.46	68.82	91.10	80.94	85.72	98.84	93.47	96.08	82.79
ETSformer	87.44	79.23	83.13	85.13	84.93	**85.03**	92.25	55.75	69.50	90.02	80.36	84.91	**99.31**	85.28	91.76	82.87
FEDformer	87.95	82.39	85.08	77.14	80.07	78.57	90.47	58.10	70.76	90.17	96.42	93.19	97.31	97.16	97.23	84.97
LightTS	87.10	78.42	82.53	82.40	75.78	78.95	**92.58**	55.27	69.21	91.98	94.72	93.33	98.37	95.97	97.15	84.23
DLinear	83.62	71.52	77.10	84.34	85.42	84.88	92.32	55.41	69.26	80.91	95.30	87.52	98.28	89.26	93.55	82.46
Stationary	88.33	81.21	84.62	68.55	**89.14**	77.50	89.37	59.02	71.09	68.03	96.75	79.88	97.82	96.76	97.29	82.08
Autoformer	88.06	82.35	85.11	77.27	80.92	79.05	90.40	58.62	71.12	89.85	95.81	92.74	99.08	88.15	93.29	84.26
Pyraformer	85.61	80.61	83.04	83.81	85.93	84.86	92.54	57.71	71.09	87.92	96.00	91.78	71.67	96.02	82.08	82.57
Anomaly Transformer	88.91	82.23	85.49	79.61	87.37	83.31	91.85	58.11	71.18	72.51	**97.32**	83.10	68.35	94.72	79.40	80.50
Informer	86.60	77.23	81.65	81.77	86.48	84.06	90.11	57.13	69.92	70.29	96.75	81.43	64.27	96.33	77.10	78.83
Reformer	82.58	69.24	75.32	85.51	83.31	84.40	90.91	57.44	70.40	72.50	96.53	82.80	59.93	95.38	73.61	77.31
LogTransformer	83.46	70.13	76.21	73.05	87.37	79.57	89.15	57.59	69.97	68.67	97.32	80.52	63.06	98.00	76.74	76.60
Transformer	83.58	76.13	79.56	71.57	87.37	78.68	89.37	57.12	69.70	68.84	96.53	80.37	62.75	96.56	76.07	76.88